Title
EXCITED-STATE PROTON TRANSFER STUDIES: INFLUENCE OF THE SOLVENT ON THE REACTION DYNAMICS

Author
Brown, W.T.

Publication Date
1986-08-01

Lawrence Berkeley Laboratory
UNIVERSITY OF CALIFORNIA

CHEMICAL BIODYNAMICS DIVISION

EXCITED-STATE PROTON TRANSFER STUDIES:
INFLUENCE OF THE SOLVENT ON THE REACTION DYNAMICS

W.T. Brown
(Ph.D. Thesis)

August 1986

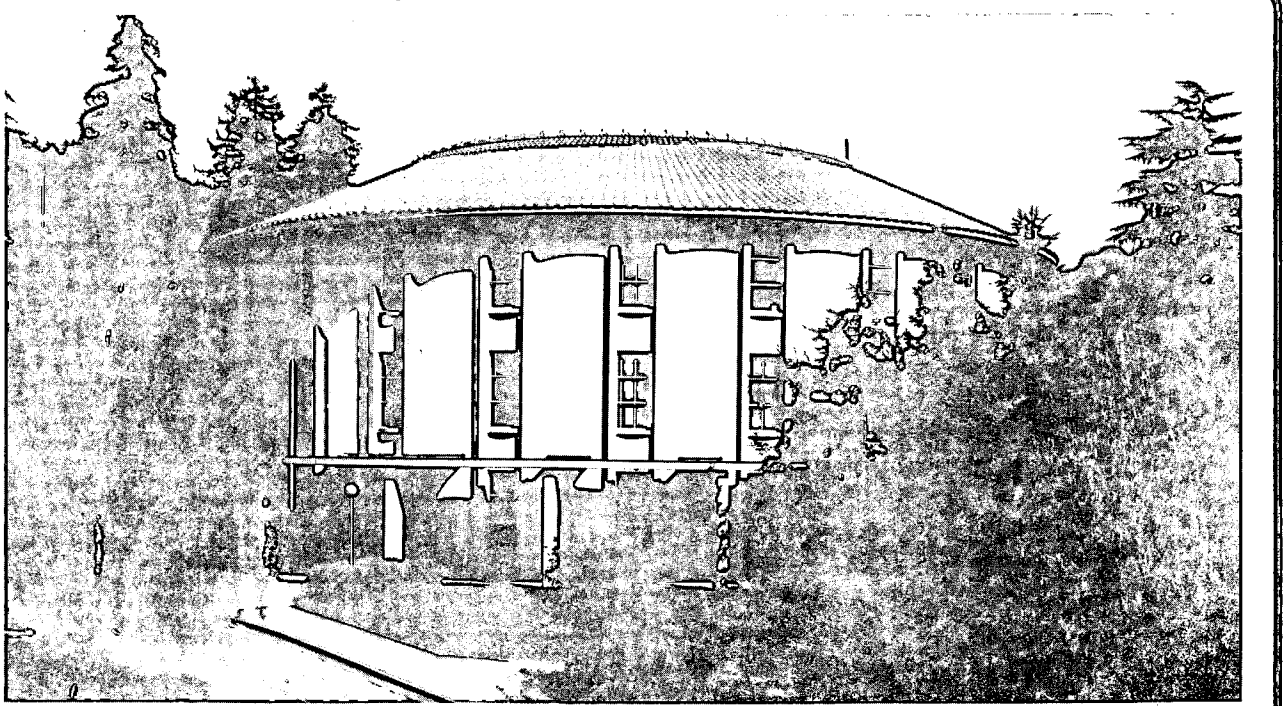

Prepared for the U.S. Department of Energy under Contract DE-AC03-76SF00098

LBL-21981

DISCLAIMER

Excited-State Proton Transfer Studies: Influence of the Solvent on the Reaction Dynamics

Ward T. Brown
Ph.D. Thesis

Lawrence Berkeley Laboratory
University of California
Berkeley, California 94720

August 1986

Excited-State Proton Transfer Studies:

Influence of the Solvent on the Reaction Dynamics

Ward T. Brown

Excited-State Proton Transfer Studies: Influence of the Solvent on the Reaction Dynamics

Ward T. Brown

Abstract

In an attempt to elucidate the role played by the solvent in proton transfer reactions, the acid dissociation rate constants for the excited states of 1-naphthol and the 1-naphthylammonium cation in H_2O have been determined using a combination of picosecond and steady-state fluorescence techniques. The rate constants have been measured over the temperature range 10 °C - 80 °C and as a function of NaCl added from 0 M - 4.8 M NaCl. The temperature studies show that the rate constants cannot be described by a single activation energy. Addition of NaCl to the solutions leads to a decrease in the rate constants. A model for the proton transfer reaction is proposed which explicitly includes the role of the solvent, and the results are discussed in light of this model. The possibility of measuring proton transfer rates in non-aqueous solvents is also discussed.

Dedication

I dedicate this thesis to:

Ralph and Wanda

two very good friends.

Acknowledgements

Although this thesis carries but one name, it is important to realize that the work and ideas necessary to complete it were in reality a group effort. In particular, this work is in some sense a continuation of a project started by Steve Webb, and I have benefited tremendously from his results. Steve and Sheila Yeh were responsible for the construction of the time resolved emission system used in this work. Sheila and Cindy Buhse were kind enough to teach me how to operate the system and to show me where to kick it when it misbehaved. Cindy also deserves credit for helping me assemble and learn the intricacies of the CW spectrofluorimeter employed in this study. In addition, all of the good people mentioned above, along with the rest of the members of our group, made the somewhat less tangible but equally important contribution of teaching me just how one does research. I thank them all. Finally, a special thanks must be given to John Clark, not only for his help and guidance throughout my graduate career, but also for his patience, understanding, and continual encouragement, which are largely responsible for the completion of this thesis.

Research support for this project was provided from the Office of Energy Research, Office of Basic Energy Sciences, Chemical Sciences Division of the Department of Energy under Contract DE-AC03-76SF00098. In addition, I have received the support of a National Science Foundation Pre-Doctoral Fellowship (1979-82).

Table of Contents

List of Figures

List of Tables

Chapter 1

Introduction

The transfer of a proton from an acid to the surrounding solvent is one of the simplest and most fundamental reactions in chemistry. The widespread occurrence of such proton transfer reactions, both in nature and in the laboratory, has sparked an enormous number of studies which have yielded a wealth of information on the subject. Yet despite the apparent simplicity of the acid dissociation reaction, the efforts thus far have failed to answer some important questions. All reactions, when studied in sufficient detail, reveal themselves to be quite complex. Proton transfer reactions are no exception. For example, the exact role of the solvent, both as the proton acceptor and in the myriad interactions that result in solvation, is not completely understood. The goal of this thesis is to examine the mechanism and kinetics of proton transfer reactions in an attempt to discern some of the details concerning the participation of the solvent.

To date, few studies along these lines have been completed.[1-5] A major reason for the current lack of knowledge of the solvent's role in proton transfer reactions is the extreme rapidity of most reactions in this class. Until the recent advent of perturbation techniques only the slowest reactions, usually involving carbon acids, could be examined using direct, time resolved kinetic analysis. Since most solvent motions occur on a time scale of 10^{-10} sec or shorter, the more common oxygen and nitrogen acids, whose deprotonation reactions usually have small activation barriers, are most likely to show the influence of the solvent. Perhaps the best chance of elucidating the importance of the solvent in proton transfer reactions is to study a reaction which proceeds at a rate comparable to the rate of common solvent motions while varying some of the properties of the solvent. Unfortunately, even the standard perturbation methods such as temperature jump, voltage jump, and shock initiation lack the necessary time resolution for such a study. A technique based on pulsed, picosecond lasers does have the required time resolution. This

technique is known as excited-state proton transfer (ESPT) dynamics[6-8] and makes use of the fact, first recognized by Förster[9] in 1949, that many molecules exhibit markedly different acidities in their ground and excited states. The pK_a's of different electronic states often vary by as much as 10 pK units. If a molecule which is a relatively weak acid in its ground state, but a strong acid in its lowest excited state, is excited with a picosecond laser pulse of the appropriate wavelength, a non-equilibrium concentration of excited-state acid molecules will be produced. If the subsequent adiabatic deprotonation reaction can be followed by some means, the proton transfer rate can be determined. Since the reactions we will be studying occur in the excited state, the fluorescence from the various excited-state species gives us a convenient method of measuring the reactant and product concentrations as the reaction proceeds. For experimental reasons, in this study we will determine the proton transfer rates by measuring the fluorescence risetime of the basic form of the parent acid. As will be shown later, it will also be necessary to measure the fluorescence decay time and quantum yield of the excited-state base as a function of pH.

Although the first observance of excited-state proton transfer[10] occurred over fifty years ago, use of the phenomenon to measure ultrafast reaction rates is considerably more recent. Historically, one of the first uses of ESPT was to measure excited-state pK_a's using a technique known as the Förster cycle.[11] This technique, shown in Figure 1.1, makes use of energy arguments to relate the excited-state acidity constant, pK_a^*, to the ground-state acidity constant, pK_a, and spectroscopic information. The relationship is

$$pK_a^* \approx pK_a + \frac{E_{0,0}^{A} - E_{0,0}^{HA}}{2.3RT}$$

where $E_{0,0}^{HA}$ and $E_{0,0}^{A}$ are the zero point transition energies from the ground to the first excited state of the acid and its conjugate base, respectively. Despite the difficulty of determining the zero point energies from broad, structureless absorption and emission spectra, and despite the neglect of the differences in the entropy of reaction for the

ground- and excited-state reactions, the technique has been remarkably successful and has been invaluable in gaining an understanding of the variation of acidity with electronic structure. However, the determination of pK_a^* for a reaction gives no direct kinetic information about the reaction. Shortly after the Förster cycle was developed, Weller[12,13] developed a method of determining the proton transfer rate utilizing only steady-state fluorescence spectra and fluorescent lifetime data. The technique involves measuring the relative fluorescence intensity of the acid and its conjugate base as a function of pH. Unfortunately, for the faster ESPT reactions the excited-state acid's fluorescence intensity is often too weak to be measured with any reliability, hence this technique is often unsuitable for our purpose. Only recently, with the advent of ultrafast pulsed lasers, has it been possible to accurately measure ESPT rates by combining direct temporal and steady-state fluorescence measurements as we have done in this study.

Although necessary for this study, the use of excited-state reactions has some serious disadvantages. Most important among these is the introduction of competitive deactivation processes such as internal conversion and diabatic quenching by buffers and inert salts added to the solution. These additional pathways greatly complicate the kinetic analysis and care must be taken in the interpretation of kinetic data. To ensure the reliability of the results of this study, it is advantageous to utilize excited-state acids for which as much as possible is already known, and whose proton transfer reactions are among the fastest known. The molecules chosen for this study are 1-naphthol and the 1-naphthylammonium cation, the structures of which are shown in Figure 1.2. Both molecules have been the subject of thorough kinetic studies performed in H_2O at room temperature.[14-16] Their photochemical and photophysical processes are quite similar and are depicted in Figure 1.3. Excitation to the lowest excited singlet state is accompanied by a partial charge transfer from the non-bonding orbitals on the oxygen (or nitrogen) atom to the 5- and 8-positions on the naphthalene moiety.[17,18] The resulting positive charge on the hydroxyl (or amino) group results in an increase in the molecule's acidity. For both molecules

Figure 1.1 The Förster Cycle

The Förster cycle is a method of determining excited-state acidity constants from thermodynamic and spectroscopic information. The method makes the explicit assumption that the ground-state and excited-state reaction entropies are similar and cancel.

Figure 1.1

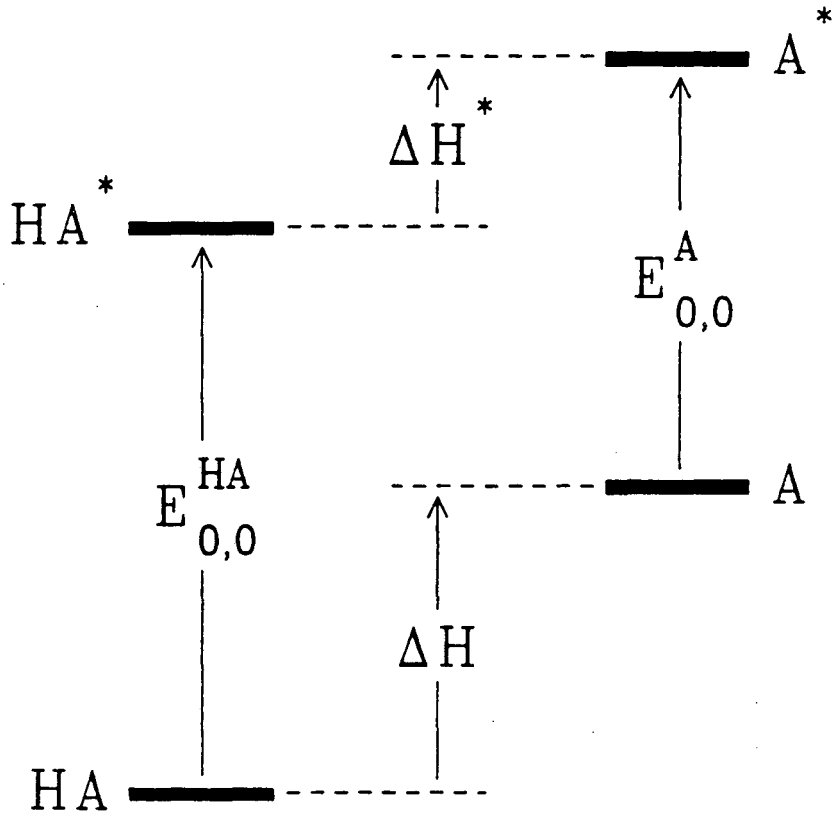

$$\Delta H^{*} = \Delta H + E^{A}_{0,0} - E^{HA}_{0,0}$$

assume $\Delta S \approx \Delta S^{*}$

$$\Delta G^{*} = \Delta G + E^{A}_{0,0} - E^{HA}_{0,0}$$

$$pK^{*}_{a} = pK_{a} + (E^{A}_{0,0} - E^{HA}_{0,0})/2.3RT$$

the excited-state acid fluoresces but undergoes fairly rapid internal conversion. Both of the excited-state conjugate bases and excited-state 1-naphthol exhibit a diabatic proton quenching process.[19-23] The forward proton transfer reaction for excited-state 1-naphthol has a rate constant, k_1, of $\sim 2 \times 10^{10}$ sec^{-1} in H_2O at 20 °C.[14] This is sufficiently fast that a variation in k_1 with the structure of the solvent is likely. While the value of k_1 for the excited-state 1-naphthylammonium ion is a factor of thirty slower than that for 1-naphthol,[15] the reaction is still quite rapid. The similarity of the two molecules makes for an interesting comparison.

Figure 1.2 Structures of 1-Naphthol and the 1-Naphthylammonium Cation

Figure 1.2

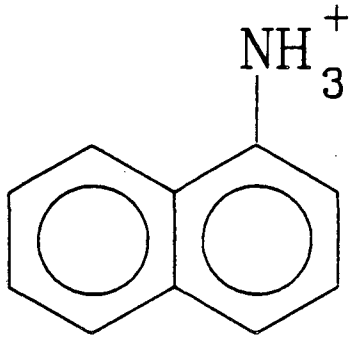

1-Naphthylammonium

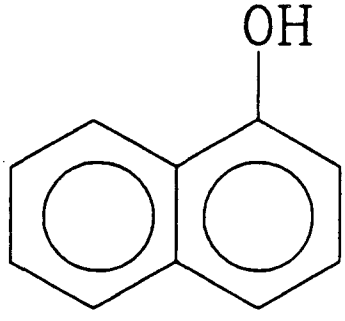

1-Naphthol

Figure 1.3 Photochemical and Photophysical Processes that Occur After Excitation of the Model Acids

The meanings of the rate constants are as follows: k_1=forward proton transfer rate, k_{-1}=reprotonation rate, k_f=rate of fluorescence, k_{nr}=non-radiative decay rate, k_q=diabatic proton quenching rate. The values listed are for the reaction in H_2O at 25 °C.

Figure 1.3

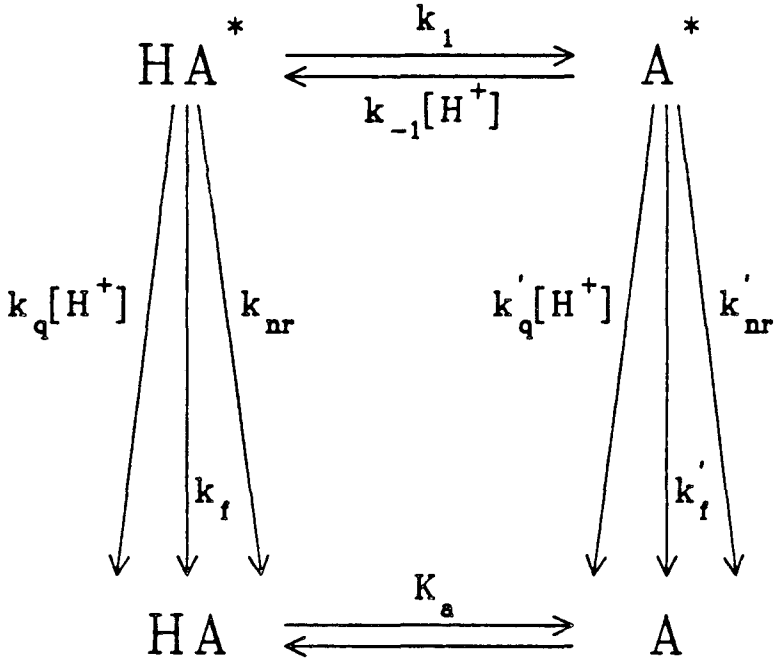

	1-Naphthol[14]	1-Naphthylammonium[15]
k_1	25	1.3
k_{-1}	68	0.12
k_q	6	–
k'_q	33	8.9
$k_f + k_{nr}$	6.8	
$k'_f + k'_{nr}$	0.13	
pK_a	9.2	3.9
pK_a^*	0.4	−1.0

The units for all of the unimolecular and bimolecular rate constants are ns^{-1} and $ns^{-1}M^{-1}$, respectively.

Chapter 2

Experimental

As mentioned in Chapter 1, the determination of the proton transfer rates requires both temporal and steady-state fluorescence measurements. The time dependence of the fluorescence signals was determined with the picosecond time-resolved emission system shown in Figure 2.1. The light source for the system was an active/passive mode-locked Nd^{3+}/YAG laser (Quantel International YG400) operated at 10 Hz. The laser produced trains of ~35 ps (FWHM) pulses at its fundamental of 1064 nm. A single pulse was isolated from the train with a pulse selector (Quantel International PF302) consisting of a Pockels cell sandwiched between two crossed Glan-Taylor polarizing prisms. The single pulse was then amplified in one or two Nd^{3+}/YAG amplifiers (Quantel International SF411-07). A small portion of the pulse was split off to a photodiode and used to trigger the detection electronics. The remainder was frequency doubled in a KDP crystal to produce the second harmonic at 532 nm. The 532-nm pulse was then itself frequency doubled in a second KDP crystal to produce the fourth harmonic at 266 nm. The fourth harmonic had a temporal width of ~25 ps (FWHM). The fundamental and harmonics were separated in a Pellin-Broca prism. A portion of the 266-nm pulse was split off and sent into the detection system to serve as a time marker, while the remainder was passed through a Glan-Taylor prism to ensure vertical polarization and then focused into the sample with a cylindrical lens. Emission was collected at 90° with respect to the excitation beam and was passed through a long wavelength pass filter (Corning CS 3-70) to remove scattered laser light and the fluorescence from the excited-state acid. The remaining fluorescence, which was from the conjugate base, was sent through a second polarizing prism set at the magic angle with respect to vertical before being sent into the detection system to remove any time dependance due to rotational reorientation of the sample. The detection system consisted of a streak camera (Hadland Photonics

Imacon 500) coupled to a cooled, intensified, 1024 channel diode array (Tracor-Northern IDARSS). The raw data was transferred to a microcomputer (Digital Equipment Corp. LSI 11/73) for correction and storage. Each final data set was the sum of the data from between 300 and 700 individual laser shots. Due to timing jitter in the firing of the streak camera the emission profiles did not always begin in the same channel of the diode array. The timing pulse mentioned earlier was used to shift the data from individual laser shots prior to the addition. The streak rate of the streak camera was nonuniform across the diode array and the nonuniformity was corrected for by calibration of the camera with an etalon. The sensitivity of the diode array was also nonuniform and was corrected daily by measuring its response to a fluorescent standard with a single, well-known decay time. The fluorescent standards were chosen to have decay times a least a factor of six longer than the total time across the diode array so that the measured fluorescence intensity changed very slowly on the time scale used. Details of the detection system and the corrections used may be found elsewhere.[24] The system's overall time resolution was 10 ps and could be used to monitor processes whose time constants ranged from 10 ps to ~30 ns. The time dependent fluorescence data was analysed on a VAX 11/780. Fluorescence lifetimes were determined using a linear least squares routine, while the risetimes were calculated using a convolute and compare technique in conjunction with the simplex method of residuals minimization.[25] Use of the timing marker as the pulse model in the convolution allowed the determination of risetimes with time constants as small (or smaller) than the laser pulse width.

Steady-state fluorescence spectra were taken on a Spex Fluorolog II spectrofluorimeter outfitted with an in-house data aquisition system. The fluorimeter was equipped with a Rhodamine B quantum reference detector to correct for fluctuations in the lamp intensity. The wavelength dependence of the fluorimeter was corrected by calibration with a standard lamp (Optronics Laboratories 245C). The temperature of the samples for both the time dependent and steady-state measurements was regulated using a refrigerated

Figure 2.1 Diagram of Picosecond Time-Resolved Emission System

The abbreviations used are: SHG for second harmonic generating crystal, FHG for fourth harmonic generating crystal, BS for beam splitter, GT for Glan-Taylor polarizing prism, L for lens, and F for filter.

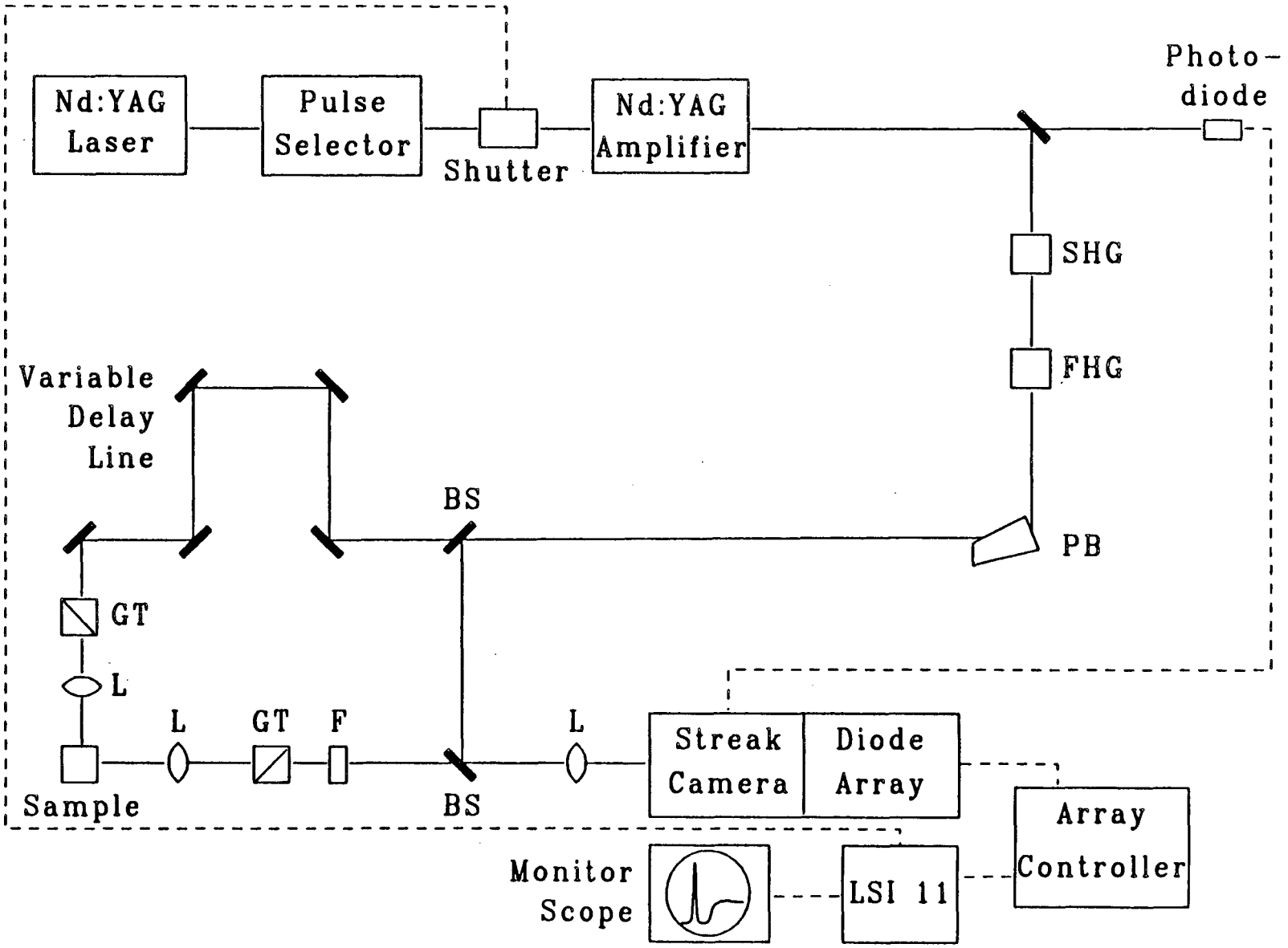
Nd:YAG Laser
Pulse Selector
Shutter
Nd:YAG Amplifier
Photo-diode
SHG
FHG
Variable Delay Line
BS
PB
GT
L
L
GT
F
L
Sample
BS
Streak Camera
Diode Array
Array Controller
Monitor Scope
LSI 11

Figure 2.1

recirculating bath (Neslab RTE-5B). Sample temperatures were determined to an accuracy of ±0.5 °C with an iron-constantan thermocouple referenced at 0 °C. Absorbance spectra were acquired with a Varian UV/Visible spectrophotometer (model 2300).

1-Naphthol (MCB Chemicals) was purified by recrystallization from CCl_4 followed by sublimation. The purified 1-naphthol was stored in the dark. 1-Naphthylamine (Aldrich) was purified by recrystallization from a 1-propanol/H_2O mixture followed by two sublimations. The purified 1-naphthylamine was stored in the dark under dry nitrogen. Water from several sources was used for the experiments; the results were independent of the source of water. The majority of the experiments used steam distilled water (Alhambra). Methanol, acetonitrile, dimethylformamide, and dimethylsulfoxide were purchased as spectral grade quality and were used without further purification. Triethylamine and N-methylformamide were distilled over CaO at reduced pressure (~200 torr). All samples were thoroughly degassed by successive freeze-pump-thaw cycles and then covered with 1 atm of dry nitrogen. Samples were generally made the day of use but samples allowed to stand several days showed no sign of decomposition and gave the same results as the fresh samples. Sample concentrations of approximately 5×10^{-4} M were used for the temporal measurements, while the steady-state measurements employed sample concentrations between 1×10^{-5} and 5×10^{-5} M. Solution pH was adjusted by the addition of NaOH or H_2SO_4.

All experiments were repeated between 3 and 6 times; the majority of the experiments were repeated four times. The uncertainties are reported as the 90% confidence levels. The method used to calibrate the time base of the streak camera system introduced a systematic error of up to 10% in all of the temporal measurements. This error is not included in the uncertainties reported.

Chapter 3

Results and Discussion

Absorption and fluorescence spectra for 1-naphthol and 1-naphthylamine are shown in Figures 3.1 and 3.2, respectively. Evidence of the ESPT reaction can be seen by the variation of these steady-state spectra with solution pH. At 20 °C in H_2O, the pK_a's of 1-naphthol and the 1-naphthylammonium ion are 9.2 and 3.9, respectively. Solutions with a pH two or more units larger than the ground-state pK_a will consist primarily of the conjugate base. As expected, excitation of such solutions produces fluorescence solely from the basic form of the molecule. Solutions with a pH several units below the sample's pK_a will consist primarily of the acidic form of the molecule. If in addition the solution pH is larger than the molecule's excited-state acidity constant, pK_a^*, then electronic excitation will be followed by dissociation of the acidic proton. Fluorescence will then be observed from both the undissociated acid and its conjugate base under these conditions.

Unfortunately, the relative fluorescence intensities of the acidic and basic forms are not in themselves a measure of the rate of proton transfer. As mentioned in Chapter 1 and as shown in Figure 1.3, there are a number of chemical and physical processes that determine the quantum yields of emission for the acid/base pair. A general technique to extract the ESPT rate constants based on a combination of temporal and quantum yield measurements is required. Such a technique is outlined below. Refer to Figure 1.3 for a definition of the various rate constants used.

If a solution containing only the acidic form of the molecule in its ground electronic state is subjected to an instantaneous excitation pulse, the concentrations of the excited-state acid, HA^*, and the excited-state conjugate base, A^*, will obey Eqs. (1) and (2)

$$\frac{d[HA^*]}{dt} = k_{-1}[H^+][A^*] - (k_1 + k_f + k_{nr} + k_q[H^+])[HA^*] \qquad (1)$$

Figure 3.1 Absorbance and Fluorescence Spectra of 1-Naphthol and the 1-Naphtholate Anion in H_2O

The solid lines represent data taken from samples containing 1-naphthol while the dashed lines represent data taken from samples containing the 1-naphtholate anion. The fluorescence from excited-state 1-naphthol has a maximum at 360 nm and appears as a shoulder on the fluorescence peak of the 1-naphtholate anion created by ESPT.

Figure 3.1

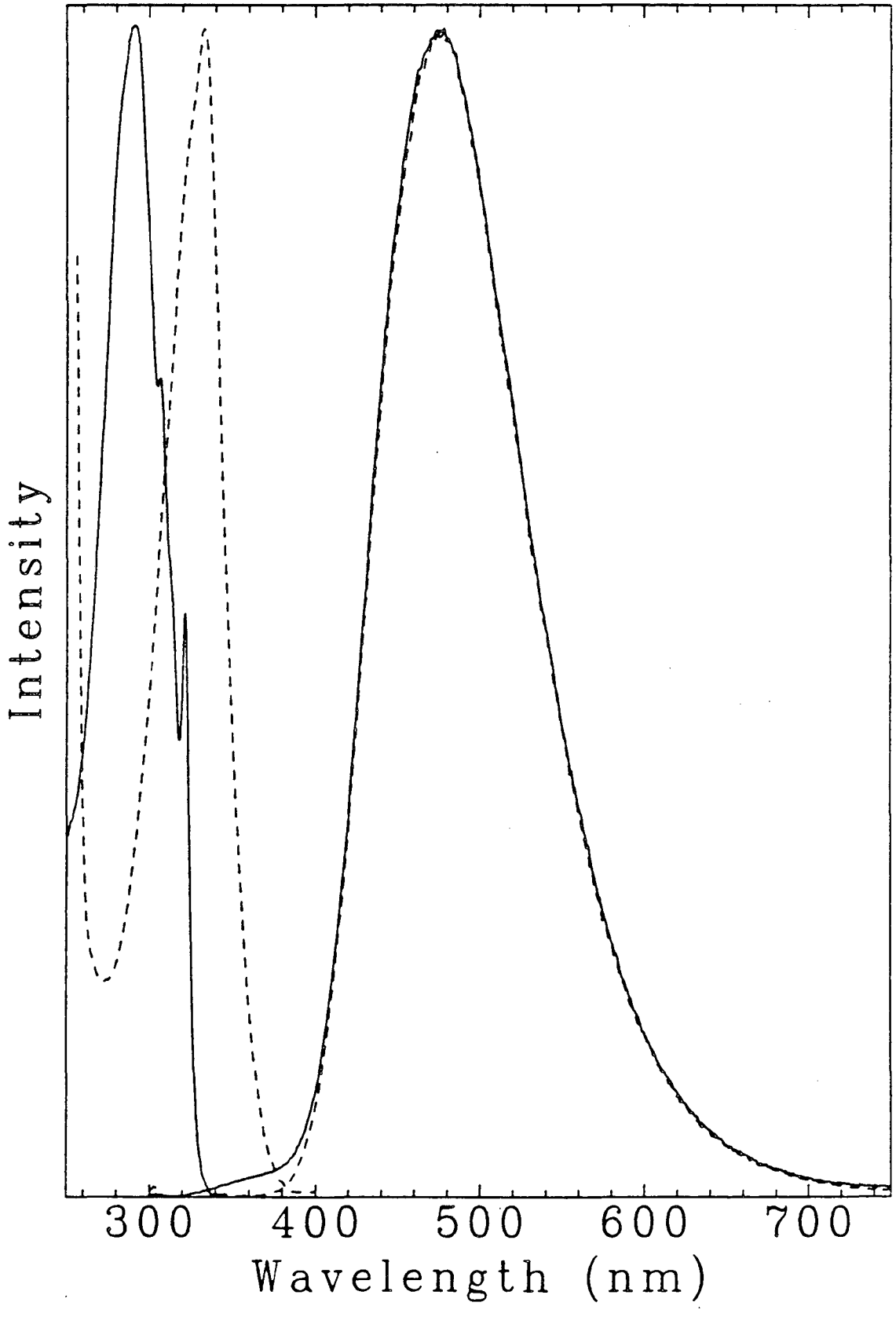

Figure 3.2 Absorbance and Fluorescence Spectra of the 1-Naphthylammonium Cation and 1-Naphthylamine in H_2O

The solid lines represent data taken from samples containing the 1-naphthylammonium cation while the dashed lines represent data taken from samples containing 1-naphthylamine. The fluorescence from the 1-naphthylammonium cation has a maximum at 330 nm while 1-naphthylamine has a fluorescence maximum at 445 nm.

Figure 3.2

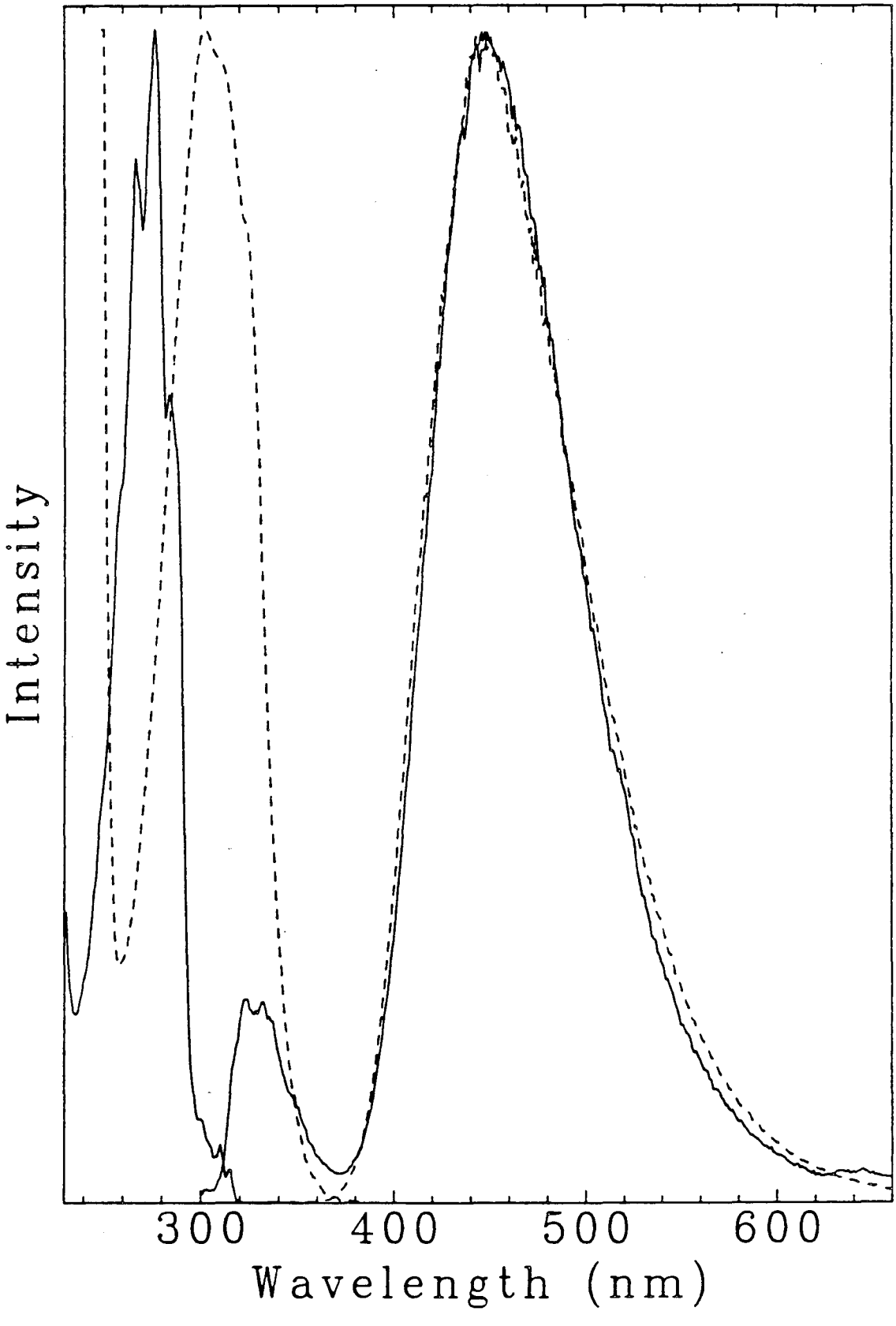

$$\frac{d[A^*]}{dt} = k_1[HA^*] - (k_{-1}[H^+] + k'_f + k'_{nr} + k'_q[H^+])[A^*]. \quad (2)$$

These coupled differential equations can be solved to give

$$[HA^*] = \frac{[HA^*]_0}{(G_1 - G_2)}[(a_1 - G_1)e^{-G_1 t} + (G_1 - a_1)e^{-G_2 t}] \quad (3)$$

$$[A^*] = \frac{[HA^*]_0}{(G_1 - G_2)}[e^{-G_2 t} - e^{-G_1 t}], \quad (4)$$

where

$$G_1 \equiv .5[(a_1 + a_2) + \sqrt{(a_1 - a_2)^2 + 4k_{-1}k_1[H^+]}], \quad (5)$$

$$G_2 \equiv .5[(a_1 + a_2) - \sqrt{(a_1 - a_2)^2 + 4k_{-1}k_1[H^+]}], \quad (6)$$

$$a_1 \equiv k_1 + k_f + k_{nr} + k_q[H^+], \quad (7)$$

$$a_2 \equiv k_{-1}[H^+] + k'_f + k'_{nr} + k'_q[H^+], \text{ and} \quad (8)$$

$$[HA^*]_0 \equiv \text{initial concentration of } HA^*.$$

In terms of measurable quantities, $1/G_1$ is the risetime and $1/G_2$ the falltime of fluorescence from A^*. It is also possible to determine G_1 and G_2 by fitting the fluorescence decay curve of HA^* to two exponentials, but experimental conditions make this method less accurate and it was not used for quantitative purposes. As will be seen below, if the pH of the solution is chosen properly, terms involving $k_{-1}[H^+]$ may be neglected to a good approximation, and Eqs. (5) and (6) can be simplified to

$$G_1 \approx a_1 \quad (9)$$

$$G_2 \approx a_2. \quad (10)$$

Turning our attention to steady-state measurements, for any solution with $pH \ll pK_a$ we can write the following expressions for the concentrations of the acidic and basic forms:

$$\frac{d[HA^*]}{dt} = k_{-1}[H^+][A^*] + I - (k_1 + k_f + k_{nr} + k_q[H^+])[HA^*] \quad (11)$$

$$\frac{d[A^*]}{dt} = k_1[HA^*] - (k_{-1}[H^+] + k'_f + k'_{nr} + k'_q[H^+])[A^*], \tag{12}$$

where I represents the rate of production of HA* by excitation of the ground-state acid. In a steady-state experiment, both [HA*] and [A*] reach constant values shortly after the onset of excitation and Eqs. (11) and (12) may be rewritten as

$$k_{-1}[H^+][A^*] - (k_1 + k_f + k_{nr} + k_q[H^+])[HA^*] = -I \tag{13}$$

$$-(k_{-1}[H^+] + k'_f + k'_{nr} + k'_q[H^+])[A^*] + k_1[HA^*] = 0. \tag{14}$$

Simultaneous solution of the linear equations for the steady-state acid and base concentrations yields

$$[HA^*] = \frac{a_2 I}{a_1 a_2 - k_1 k_{-1}[H^+]} \tag{15}$$

$$[A^*] = \frac{k_1 I}{a_1 a_2 - k_1 k_{-1}[H^+]} \tag{16}$$

where use of Eqs. (7) and (8) has been made. From Eq. (16), the fluorescence quantum yield of the basic form may be found as

$$\Phi_A = \frac{k_1 k'_f}{a_1 a_2 - k_1 k_{-1}[H^+]}. \tag{17}$$

For a solution with only the basic form present, ie, if pH$\gg$pK_a, the fluorescence quantum yield of the basic form can be expressed as

$$\Phi^0_A = \frac{k'_f}{a^0_2}, \tag{18}$$

where the superscripts indicate the requirement that pH$\gg$pK_a. Combining Eqs. (17) and (18) yields

$$\frac{\Phi_A}{\Phi^0_A} = \frac{a^0_2 k_1}{a_1 a_2 - k_1 k_{-1}[H^+]}. \tag{19}$$

Once again, if we choose the pH of the solution properly we can ignore the terms involving $k_{-1}[H^+]$ in Eq. (19) and obtain the somewhat simpler expression

$$\frac{\Phi_A}{\Phi^0_A} = \frac{k_1}{a_1}\frac{a^0_2}{a_2}. \tag{20}$$

Note that a_2 and a_2^0 are not equal and do not cancel in Eq. (20) due to their explicit dependence on $[H^+]$. It is possible that a_2 and a_2^0 also differ due to a dependance of k'_{nr} on the concentration of the counter ions introduced into the solution when adjusting the pH. The ratio a_2^0/a_2 can be determined quite easily; a_2 may be obtained from Eq. (10) and, as defined, a_2^0 is simply the fluorescence decay rate of a sample with the same pH as that used to find Φ_A^0. Combining Eqs. (20) and (9) we arrive finally at the expression for k_1,

$$k_1 = G_1 \frac{\Phi_A}{\Phi_A^0} \frac{a_2}{a_2^0}, \tag{21}$$

where, again, $1/G_1$ is the risetime of the fluorescence of the basic form, Φ_A and Φ_A^0 are the fluorescence quantum yields of the basic form in solutions initially containing only the acidic and basic forms, respectively, and a_2 and a_2^0 are the fluorescence decay rates of the basic form in solutions initially containing only the acidic and basic forms, respectively.

In the derivation of Eq. (21) it was assumed only that there exists some pH for which both of the following are true: 1) only the acidic form is initially present in the solution, ie., $pH \ll pK_a$, and 2) terms involving $k_{-1}[H^+]$ may be neglected in comparison with terms such as a_1 and a_2. For 1-naphthol the pK_a is 9.2 and neutral solutions will satisfy the first requirement. At pH 7 the proton concentration is so small that all $[H^+]$ dependent terms may be neglected, as can be seen by examining the magnitudes of the rate constants listed in Figure 1.3. For the 1-naphthylammonium cation, the pK_a is 3.9, so the solution must be acidified to at least pH 2 to satisfy the first requirement. At this low pH it is not in general valid to ignore $[H^+]$ dependent terms. However, the term $k_{-1}[H^+]$ never appears apart from the term $k'_q[H^+]$, and $k_{-1}/k'_q \approx .01$. Neglect of $k_{-1}[H^+]$ will not cause a significant error at any pH.

Examples of data acquired with the streak camera system are shown in Figures 3.3 and 3.4. Figure 3.3 shows a typical data set used to determine fluorescence risetimes,

in this case for 1-naphthol. The feature at channel #150 is the timing marker used in convoluting the data. Figure 3.4 shows a data set used to determine the fluorescence decay time of 1-naphthylamine at pH 7, ie., a_2^0. As the figures show, the streak camera system is capable of acquiring data with quite good signal to noise ratios, even when very fast risetimes are being measured. The results are sensitive to the diode array sensitivity correction mentioned in Chapter 2 and vary somewhat from day to day. These variations are the major source of uncertainty in the G_1, a_2, and a_2^0 values. Since k_1 depends only on relative quantum yields, Φ_A/Φ_A^0 was determined by taking the ratios of the intensities of the base fluorescence, normalized to the solution's absorbance, for samples containing only the acidic form and only the basic form. It is important to excite the samples at the isoabsorbance wavelength for the acid/base pair for the normalization to be strictly valid. However, at this wavelength, the absorbance of the basic form is changing rapidly and errors in measuring the absorbances account for most of the uncertainties listed for the quantum yield measurements.

Using Eq. (21) the ESPT rate constant for aqueous 1-naphthol was determined as a function of temperature and concentration of NaCl added to the solution, while for the aqueous 1-naphthylammonium cation, k_1 was determined as a function of temperature. The results are summarized in Tables 1-4, and in Figures 3.5-3.8. As the figures show, for 1-naphthol k_1 becomes essentially temperature independent above 50 °C in both neat H_2O and 4.8M $NaCl_{(aq)}$ while k_1 for the 1-naphthylammonium cation increases monotonically with temperature and is reasonably well described by the activated complex theory equation

$$k_1 = \frac{k_b T}{h} e^{\Delta S^{\ddagger}/R}\, e^{-\Delta H^{\ddagger}/RT}, \qquad (22)$$

where k_b is Boltzmann's constant, h is Plank's constant, and R is the ideal gas constant. Also, as shown in Figure 3.6, although the dissociation of excited-state 1-naphthol is a (pseudo) unimolecular reaction of an uncharged molecule, k_1 has a strong inverse

Figure 3.3 Fluorescence Risetime of the 1-Naphtholate Anion in H_2O

An example of the raw data from the time-resolved emission system; shown here is the rise of fluorescence from the 1-naphtholate anion in a pH 7 solution at 20 °C. The feature at channel #150 is the timing marker. For this experiment the time base was set at 0.96 ps/channel.

Figure 3.3

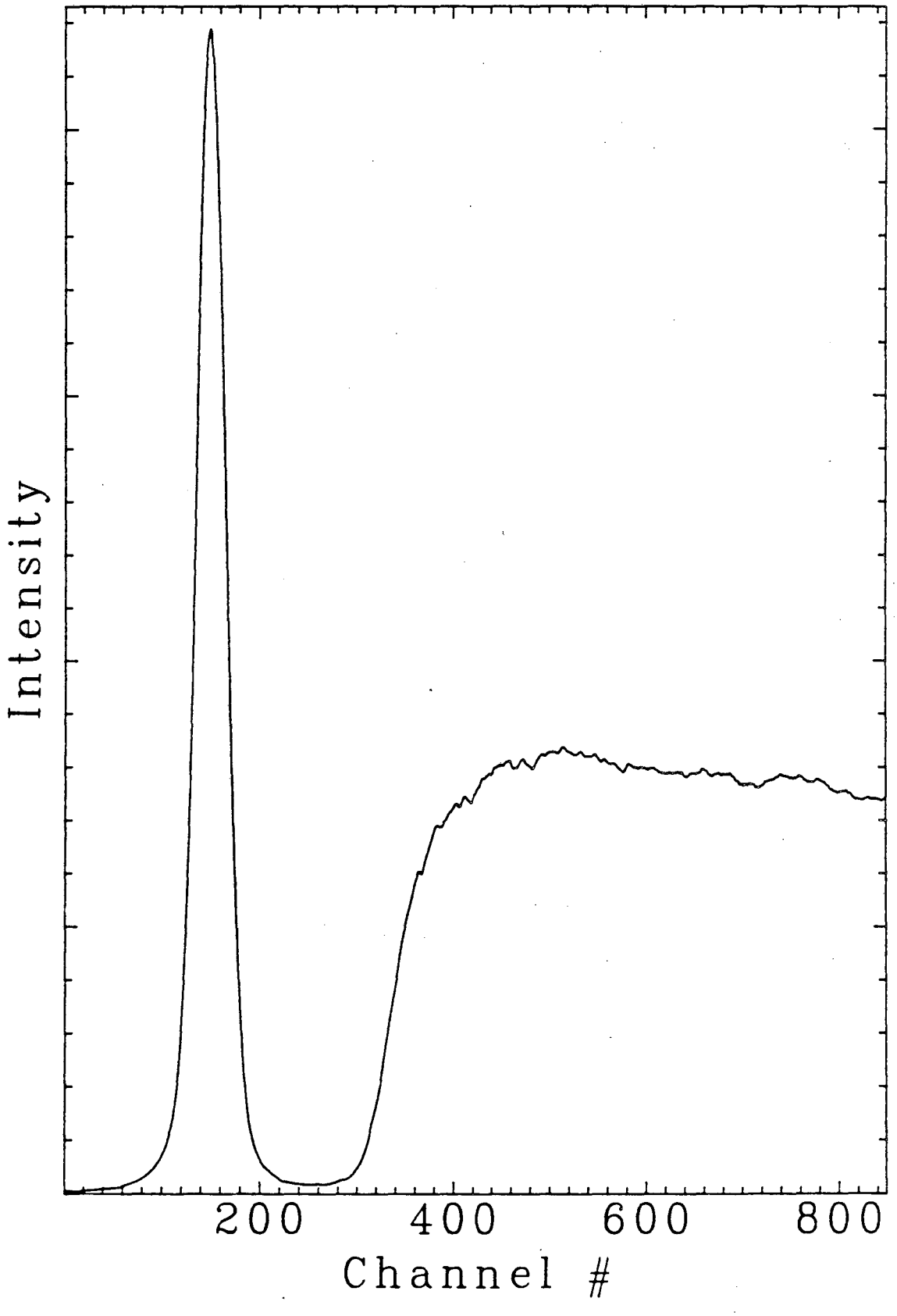

Figure 3.4 Fluorescence Falltime of 1-Naphthylamine in H_2O

An example of the raw data from the time-resolved emission system; shown here is the decay of fluorescence from 1-naphthylamine in a pH 7 solution at 20 °C. The feature at channel #50 is the timing marker. For this experiment the time base was set at 93.4 ps/channel.

Figure 3.4

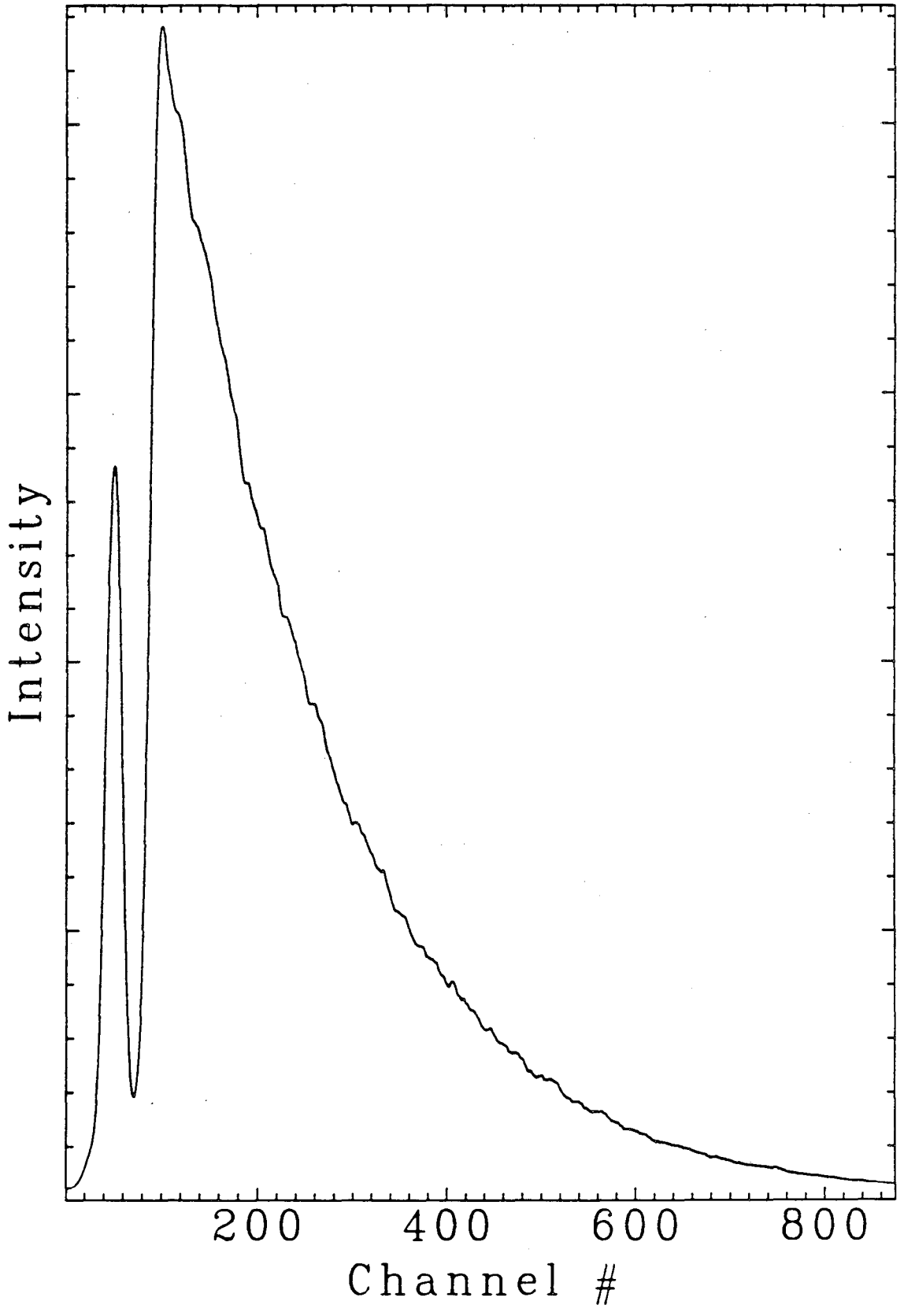

dependence on the concentration of NaCl added to the solution.

To understand at least part of the influence the solvent exerts on proton transfer reactions, we desire a simple model of the reaction dynamics that will account for the observed trends. One such model is shown in Figure 3.9. Following excitation to the reactive potential surface the molecule undergoes rapid vibrational relaxation to the bottom of the excited-state potential well. Simultaneously, the surrounding solvent molecules will begin to reorient themselves in response to any changes in the acid's dipole moment or hydrogen bonding capabilities. Studies have shown that this reorientation is also extremely rapid,[24,26] and would be predicted to be on the order of 0.1 ps for H_2O at 20 °C. Since the fastest reaction rate measured here has a half-life of around 30 ps it seems unlikely that either the acid's vibrational relaxation or the reorientation of the solvent is in any way rate limiting. It is reasonable to assume that the acidic hydrogen is strongly H-bonded to the solvent. It is well known that water and other amphoprotic solvents form H-bonded clusters in the liquid phase.[27] Although there is undoubtedly a wide distribution of cluster sizes and any given cluster probably grows and shrinks continuously and rapidly, for the sake of simplicity we will consider the acid to be H-bonded to a solvent cluster of "average" size containing n molecules. Motion of the proton along the axis of the H-bond results in proton dissociation with a rate constant of k_F. The initially formed product is an encounter complex consisting of the conjugate base and the protonated solvent cluster. This encounter complex may again react, with a rate of k_B, to give back the parent acid, or the encounter complex may break apart and the components diffuse away from each other with a rate constant k_D. If the steady-state approximation is made for the concentration of the encounter complex, this model predicts that the experimentally measured rate constant k_1 and the microscopic rate constants k_F, k_B, and k_D can be related by

$$k_1 = \frac{k_F k_D}{k_B + k_D}. \tag{23}$$

Table 1

Results for 1-Naphthol in H_2O vs. Temperature

Temp. (°C)	a_2 (ns^{-1})	a_2^0 (ns^{-1})	Φ_A/Φ_A^0	G_1 (ns^{-1})	k_1 (ns^{-1})
10	0.111±.003	0.109±.006	0.70±.01	29±3	20±2
20	0.114±.006	0.111±.005	0.69±.03	30±5	21±4
30	0.121±.003	0.117±.003	0.71±.02	33±3	25±2
40	0.126±.003	0.121±.003	0.73±.02	38±5	29±4
50	0.130±.006	0.126±.004	0.73±.02	43±8	32±6
60	0.137±.005	0.132±.007	0.75±.01	41±5	32±4
70	0.145±.007	0.138±.006	0.76±.02	41±9	33±8
80	0.156±.007	0.148±.008	0.76±.02	41±9	33±7

Table 2

Results for 1-Naphthol in H_2O vs. Concentration of NaCl

[NaCl] (M)	a_2 (ns^{-1})	a_2^0 (ns^{-1})	Φ_A/Φ_A^0	G_1 (ns^{-1})	k_1 (ns^{-1})
0.0	0.114±.006	0.111±.005	0.69±.03	30±5	21±4
1.0	0.116±.002	0.114±.003	0.71±.02	23±4	17±3
2.0	0.116±.001	0.113±.002	0.67±.02	18±3	12±2
3.0	0.116±.001	0.114±.001	0.64±.06	14±2	9±1
4.0	0.117±.001	0.112±.003	0.63±.02	11±2	7±1
4.8	0.115±.002	0.111±.004	0.62±.02	10±2	6±1

All values are for 20 °C.

Table 3

Results for 1-Naphthol in 4.8 M $NaCl_{(aq)}$ vs. Temperature

Temp. (°C)	a_2 (ns^{-1})	a_2^0 (ns^{-1})	Φ_A/Φ_A^0	G_1 (ns^{-1})	k_1 (ns^{-1})
10	0.108±.002	0.108±.004	0.62±.08	6.6±.4	4.1±.6
20	0.110±.002	0.110±.003	0.62±.05	7.0±.8	4.3±.6
30	0.111±.002	0.113±.002	0.63±.05	7.2±.7	4.5±.5
40	0.116±.002	0.116±.002	0.63±.04	8.4±1.0	5.3±.7
50	0.119±.005	0.120±.001	0.63±.04	9.5±1.0	6.0±.8
60	0.120±.003	0.122±.003	0.62±.04	9.4±1.2	5.8±.8
70	0.126±.002	0.124±.003	0.60±.05	9.5±1.2	5.8±.9
80	0.127±.004	0.129±.003	0.58±.06	9.5±1.1	5.4±.9

Table 4

Results for the 1-Naphthylammonium Cation in H_2O vs. Temperature

Temp. (°C)	a_2 (ns^{-1})	a_2^0 (ns^{-1})	Φ_A/Φ_A^0	G_1 (ns^{-1})	k_1 (ns^{-1})
10	0.18±.01	0.068±.002	0.508±.003	0.38±.03	0.52±.05
20	0.185±.003	0.065±.001	0.54±.05	0.52±.03	0.76±.09
30	0.21±.02	0.070±.002	0.56±.06	0.71±.03	1.2±.2
40	0.22±.01	0.074±.002	0.59±.07	0.90±.06	1.6±.2
50	0.24±.01	0.080±.002	0.64±.04	1.14±.03	2.2±.2
60	0.25±.02	0.082±.002	0.66±.03	1.56±.06	3.1±.3
70	0.26±.02	0.086±.003	0.68±.04	1.77±.08	3.7±.4
80	0.28±.03	0.091±.003	0.70±.06	2.01±.07	4.4±.7

Figure 3.5 Proton Transfer Rate as a Function of Temperature for 1-Naphthol in H_2O

The line drawn through the data is a fit of the data from 10 °C to 50 °C to Eq. (22). The fit parameters are $\Delta H^{\ddagger} = 1.4 \pm .8$ kcal/mole and $\Delta S^{\ddagger} = -6.3 \pm 2.6$ eu.

Figure 3.5

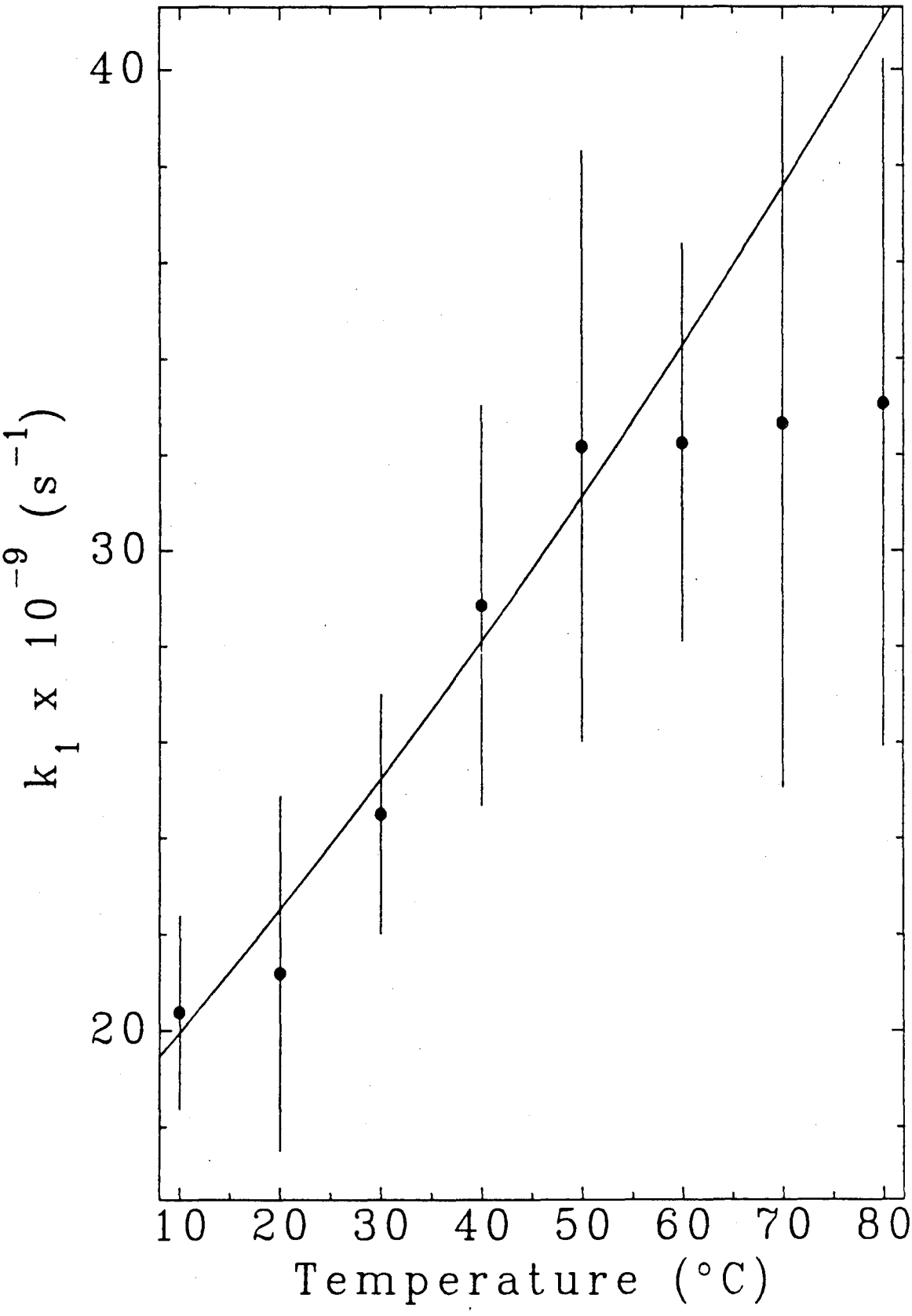

Figure 3.6 Proton Transfer Rate as a Function of Added NaCl for 1-Naphthol in H_2O

Figure 3.6

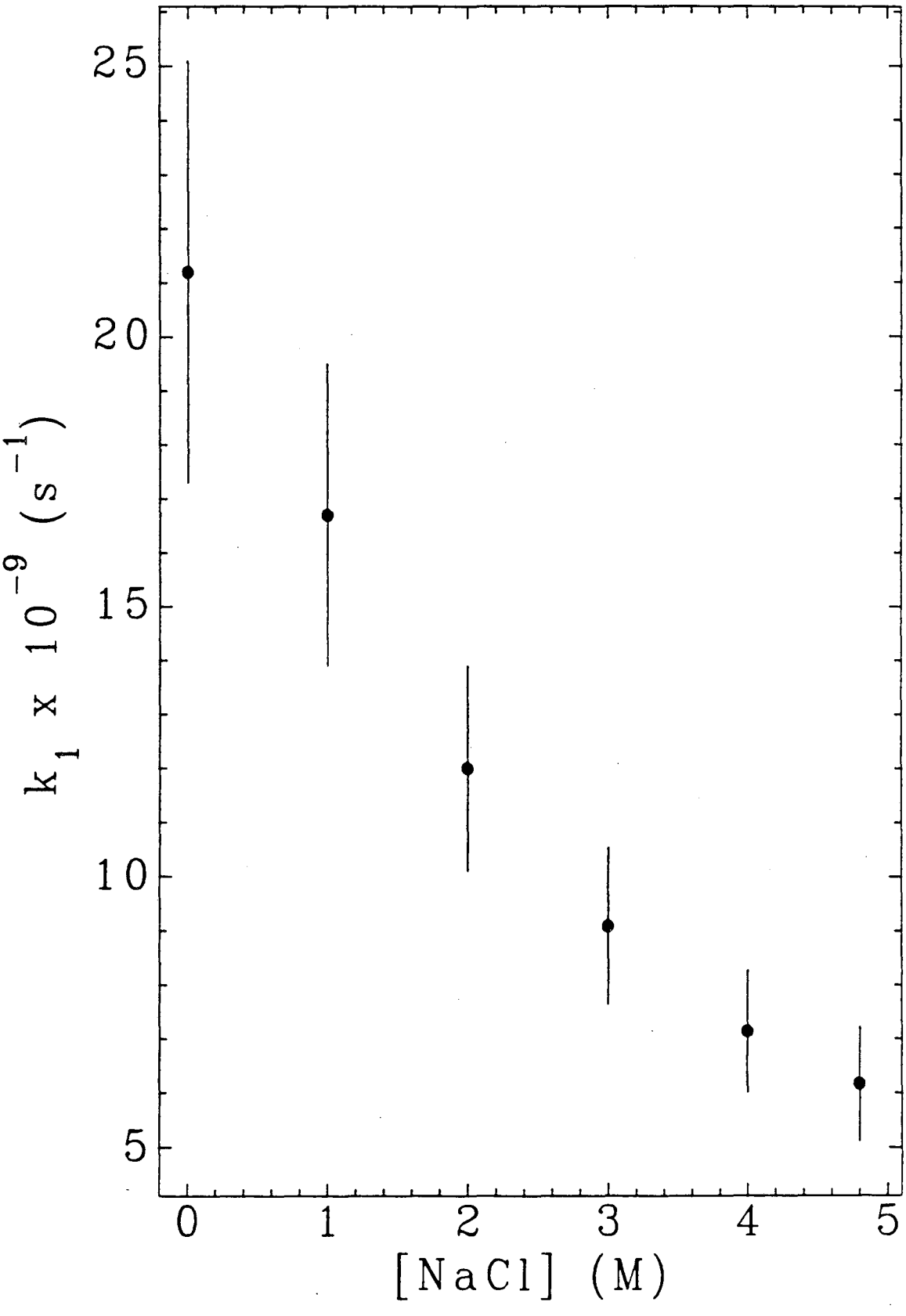

Figure 3.7 Proton Transfer Rate as a Function of Temperature for 1-Naphthol in 4.8 M $NaCl_{(aq)}$

The line drawn through the data is a fit of the data from 10 °C to 50 °C to Eq. (22). The fit parameters are $\Delta H^{\ddagger} = 1.1 \pm .8$ kcal/mole and $\Delta S^{\ddagger} = -10.5 \pm 2.7$ eu.

Figure 3.7

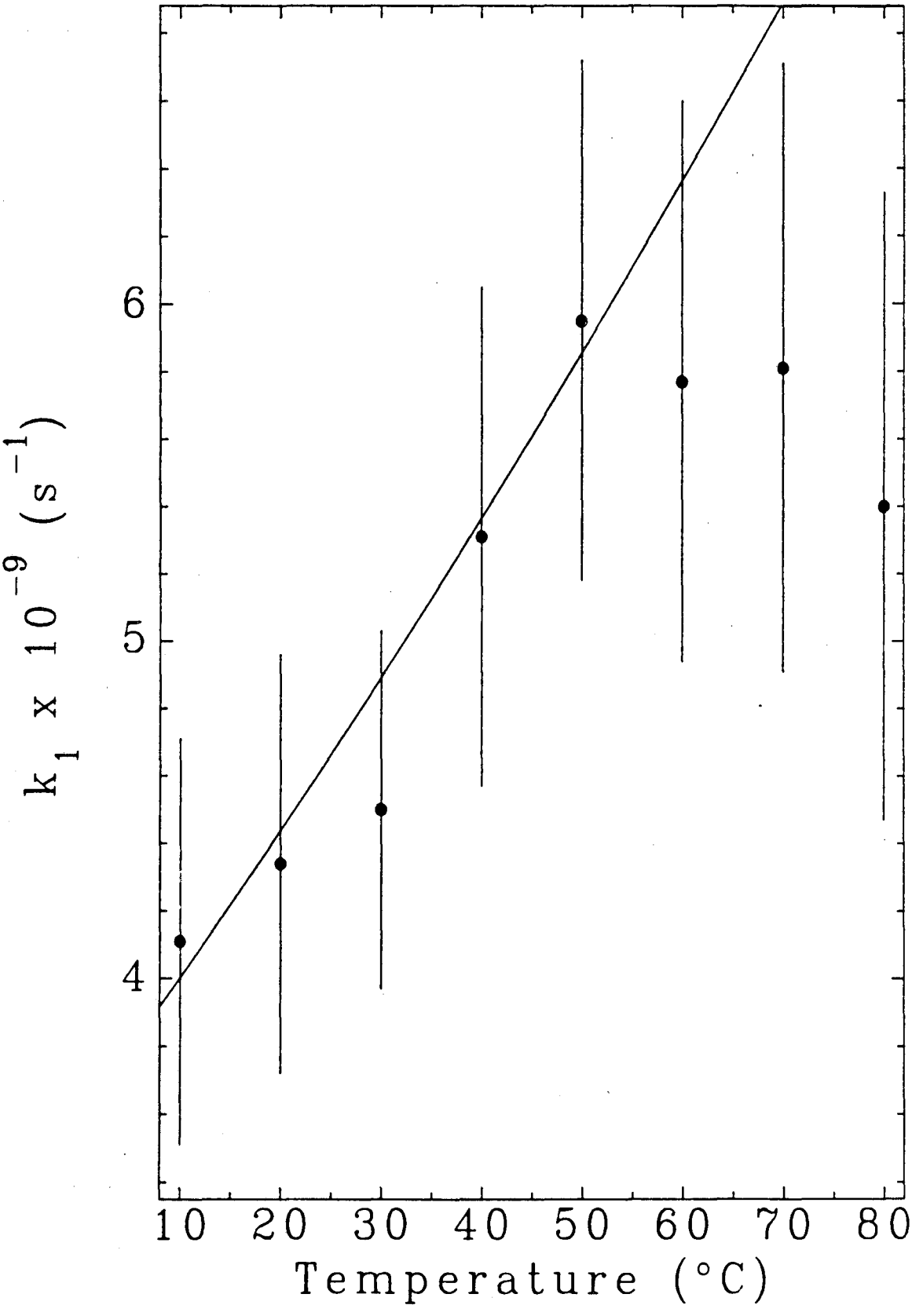

Figure 3.8 Proton Transfer Rate as a Function of Temperature for the 1-Naphthylammonium Cation in H_2O

The line drawn through the data is a fit of the data to Eq. (22). The fit parameters are $\Delta H^{\ddagger} = 5.7 \pm .3$ kcal/mole and $\Delta S^{\ddagger} = 1.5 \pm 1.0$ eu.

Figure 3.8

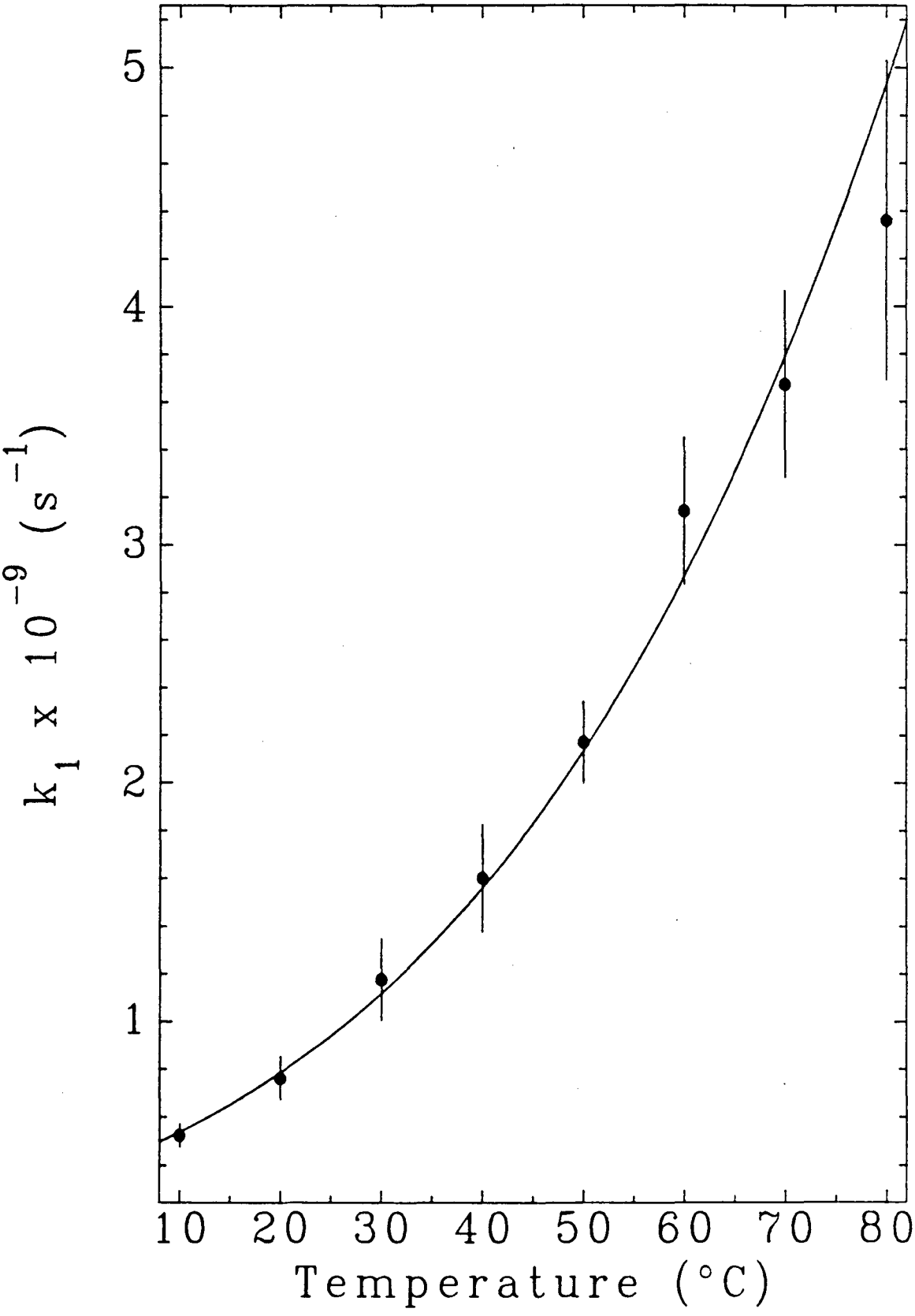

Eq. (23) may now be used to explain the results presented above.

Normally, reactions involving neutral species are not expected to display a strong salt effect. In terms of the microscopic rate constants this means that k_F should vary only slightly with salt concentration. However, k_D and k_B would be expected to show a noticeable salt effect. The strong electrostatic field exerted by the ions is known to disrupt the hydrogen bonding of the solvent in the vicinity of the ions.[27,28] As a result of this "structure breaking" effect the solvent becomes less associated than in the pure liquid. There are two effects on k_D that work in opposite directions. In amphoprotic solvents like water the proton has an abnormally high diffusion rate for a particle of its size. This large diffusion rate is attributed to a proton tunnelling mechanism where the solvated proton jumps along a network of hydrogen bonded solvent molecules,[29-32] as depicted in Figure 3.10. Disruption of the H-bonded network inhibits this tunnelling mechanism and would lead to a decrease in k_D. However, disruption of H-bonding also lowers the solvent's viscosity and the resulting increase in ordinary hydrodynamic diffusion rates will offset the decrease in k_D to some extent. From Figure 3.11, which shows the dependences of the proton diffusion coefficient and k_1 for 1-naphthol on the concentration of NaCl, we can see that a decrease in k_D probably accounts for some but not all of the variation in k_1. The remainder of the decrease in k_1 can be attributed to an increase in k_B, the backward rate constant. Gas phase experiments[33,34] and theoretical calculations[35,36] have shown that the enthalpy of solvation for the proton becomes more negative with an increase in the size of the solvating cluster. Addition of salt to the solution can be expected to decrease the average solvent cluster size. This in effect would decrease $\Delta G^{\ddagger}$ for the back reaction and lead to an increase in k_B. The model predicts that this decrease in k_1 with added inert salt should be a general one for any proton transfer reaction with $k_B \geq k_D$, ie., any reaction with a small activation barrier for the back reaction. Huppert et al.[5] have studied the effect of added inert salt on the proton transfer rates of six acids with a wide range of rate constants. Although a_1, and not k_1, was probably measured, the

Figure 3.9 A Model of the Proton Transfer Reaction

The symbols used have the following meanings: S_n is a solvent cluster composed of n solvent molecules, k_F is the initial proton transfer rate to form an encounter complex, k_B is the encounter complex's back reaction, and k_D is the rate of diffusional separation of the encounter complex to complete the overall proton transfer reaction.

Figure 3.9

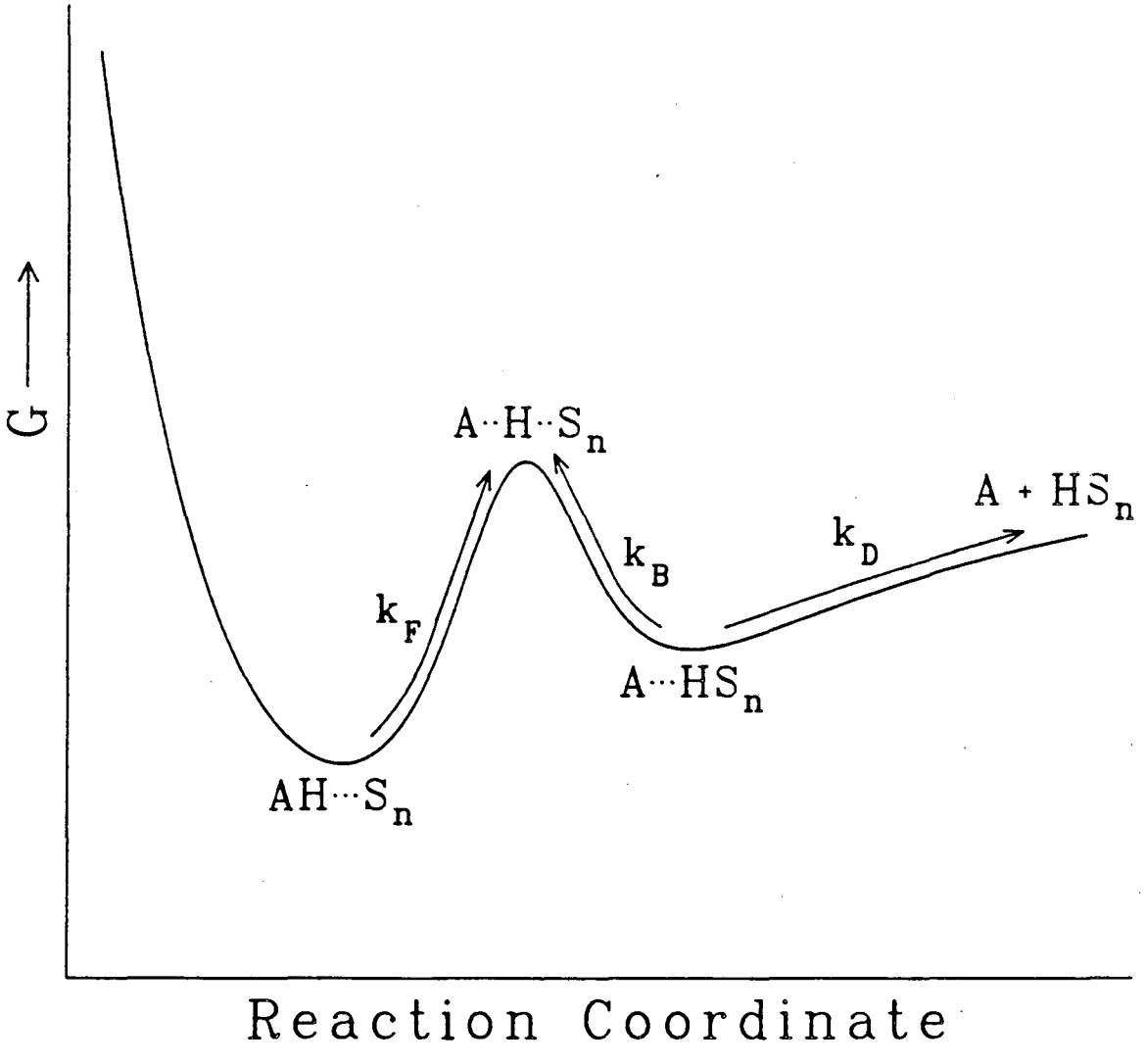

values show a similar salt effect for all of the acids studied. Huppert also attributed the decrease in dissociation rates to a break up in the water structure but did not propose a specific mechanism.

If for 1-naphthol and 1-naphthylammonium ion in H_2O $k_B \gg k_D$, Eq. (23) may be approximated as

$$k_1 \approx \frac{k_F k_D}{k_B} \tag{24}$$

and k_1 would be expected to obey Eq. (22) with $\Delta H^{\ddagger} = \Delta H_F^{\ddagger} + H_D^{\ddagger} - H_B^{\ddagger}$ and similarly for $\Delta S^{\ddagger}$. While this appears to be the case for the 1-naphthylammonium cation, Figure 3.5 shows that for 1-naphthol k_1 becomes essentially temperature independent above 50 °C. This result can be explained by considering the effect of temperature on $\Delta H_B^{\ddagger}$. While not strictly valid, it is usually assumed that enthalpies of activation are independent of temperature. However, as was mentioned in the discussion of the salt effect, $\Delta H_B^{\ddagger}$ is dependent on the solvent cluster size, which in turn is expected to decrease with temperature. The result is that $\Delta H_B^{\ddagger}$ should decrease with an increase in temperature, and consequently k_B should increase more rapidly than is normal with increasing temperatures. While this effect should be observed for all reactions that obey Eq. (24), its magnitude will depend on the size of $\Delta H^{\ddagger}$. Since the change of $\Delta H_B^{\ddagger}$ with temperature is dependent only on the solvent, the relative change in $\Delta H^{\ddagger}$ will be smaller for reactions with larger energy barriers. For the 1-naphthylammonium cation in H_2O, $\Delta H^{\ddagger}$ is found to be 5.7±.3 kcal/mole using the data from 10 °C to 80 °C. A fit of the data for 1-naphthol from 10 °C to 50 °C gives $\Delta H^{\ddagger}$ =1.4±.8 kcal/mole, while the lack of variation in k_1 above 50 °C implies that $\Delta H^{\ddagger} \approx 0$ at the higher temperatures. Since the 1-naphthylammonium ion has an activation enthalpy four times larger than that for 1-naphthol, the deviation from Eq. (22) is less apparent. However, if the data for the 1-naphthylammonium cation is split into two regions which are analysed separately, the data below 50 °C give an activation enthalpy approximately 1 kcal/mole higher than the

Figure 3.10 Mechanism of Proton Tunnelling Process in Water

In addition to ordinary hydrodynamic diffusion, in amphoprotic solvents the proton moves through the solution by "jumping" along H-bonded networks of solvent molecules.

Figure 3.10

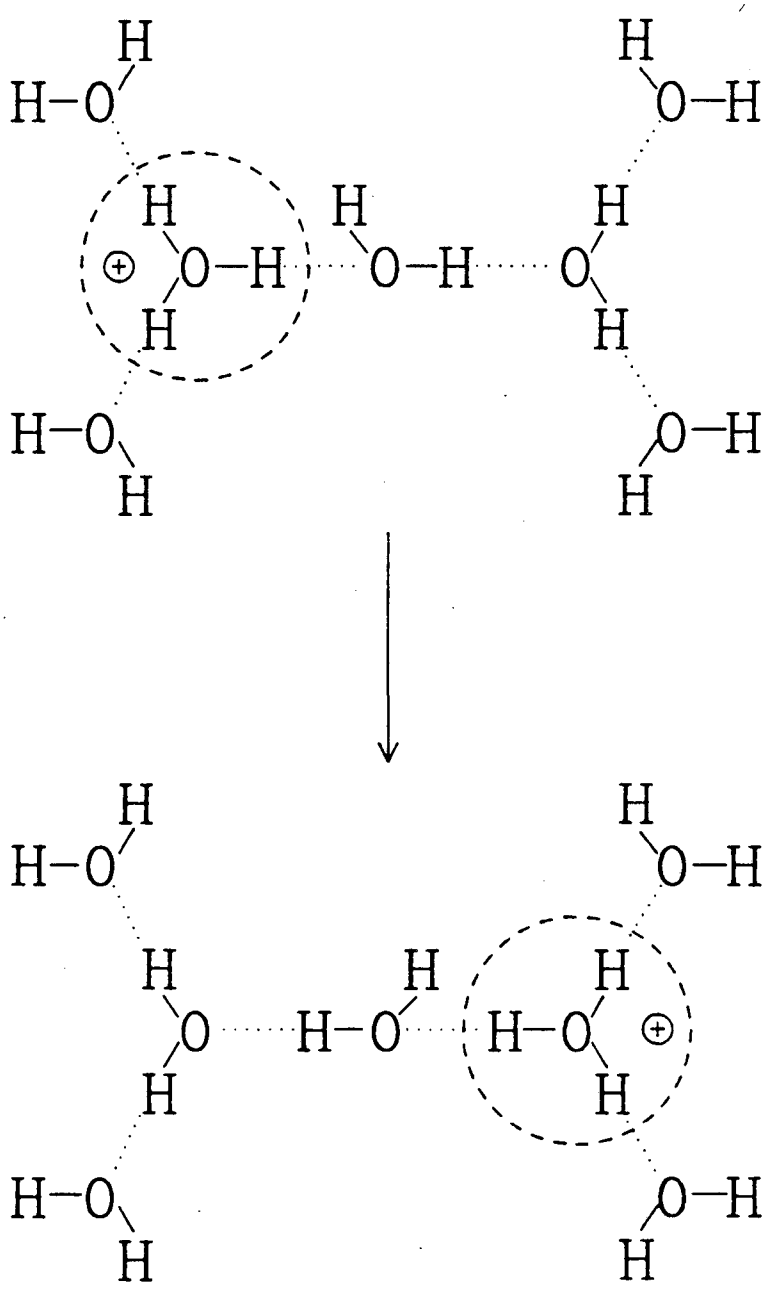

Figure 3.11 Comparison of the Proton Transfer Rate for 1-Naphthol and the Proton Diffusion Coefficient in Aqueous NaCl Solutions

The data have all been normalized to their values in neat H_2O. The open circles show the normalized proton diffusion coefficient while the solid circles show the normalized proton transfer rate of 1-Naphthol. The figure shows that a decrease in the proton diffusion rate probably accounts for some but not all of the decrease in the proton transfer rate. The proton diffusion coefficients are taken from ref. (37).

Figure 3.11

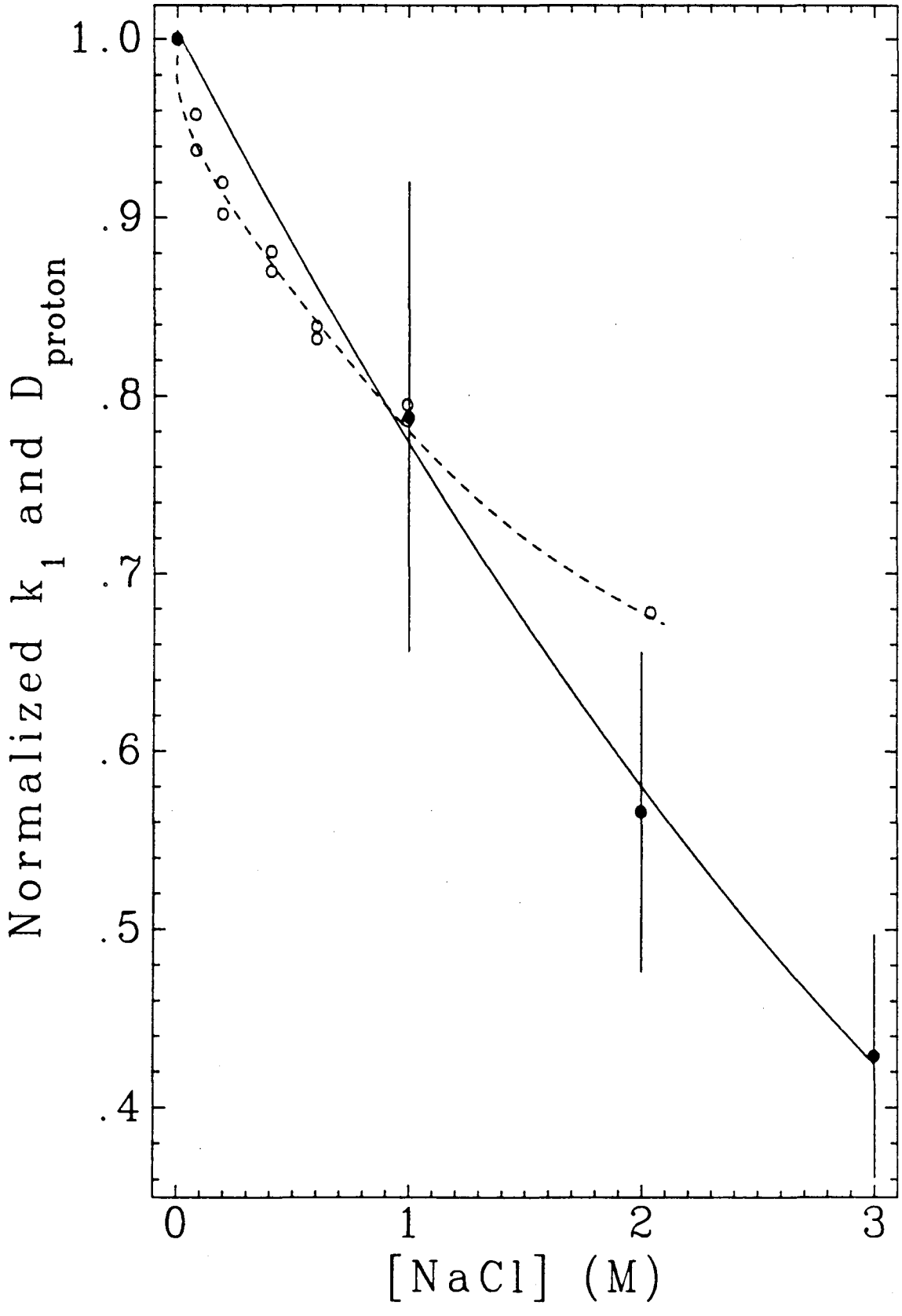

data above 50 °C, the same result that is found for 1-naphthol. It should be pointed out that the observed deviations from Eq. (22) can also be explained if k_B is not considerably larger than k_D. In this case Eq. (24) is not valid; we must use Eq. (23) and no simple expression can be written for $\Delta H^{\ddagger}$.

If the addition of salt and the increase of temperature does indeed change $\Delta H^{\ddagger}$ by reducing the average solvent cluster size, then a plot of k_1 vs. temperature in a concentrated salt solution should look similar to such a plot in the pure solvent but should give a smaller value of $\Delta H^{\ddagger}$. Such a plot for 1-naphthol in water is shown in Figure 3.7. Again above 50 °C, k_1 ceases to change with temperature. A fit of the data from 10 °C to 50 °C to Eq. (22) gives a value for $\Delta H^{\ddagger}$ of 1.1±.8 kcal/mole. While this is the predicted result, the large uncertainties in the two $\Delta H^{\ddagger}$ values limit the statistical significance of the finding.

Two results from the literature bear examination in light of these findings. The first is the effect of deuterating the solvent on k_1. Webb et al.[14] found that k_1 for 1-naphthol decreased by a factor of 3 in going from H_2O to D_2O while Huppert et al.[4] found that for 8-hydroxy-1,3,6-pyrene trisulfonate $a_1(H_2O)/a_1(D_2O)=3.5$, where it was assumed that $k_1 \approx a_1$. Replacing the acidic proton with a deuteron will lower the zero point vibrational energy along the reaction coordinate by $\sim 800 cm^{-1}$ for both the acid and the base/solvated proton encounter complex. In effect this increases both $\Delta H_F^{\ddagger}$ and $\Delta H_B^{\ddagger}$, but by roughly the same amount. The ratio k_F/k_B is not expected to show a large isotope effect. However, k_D will be smaller for reactions in D_2O compared to H_2O. The larger weight of the deuteron slows hydrodynamic diffusion and increases the effective activation barrier that the proton must tunnel through in the proton jump mechanism. Experimentally, it has been found that deuteration slows diffusion of protons in water by a factor of 1.6,[29] roughly half of the change found in k_1. The reason for this discrepancy is not clear, but one possible explanation is that the activated complex is slightly different for the forward and backward reactions. Motion of the proton along the reaction coordinate

would be essentially an asymmetric vibrational stretching mode of the activated complex, except that the motion is unbound. However, the corresponding symmetric mode is bound and its zero point energy contributes to the energy of the activated complex. If the activated complex is not symmetrical with respect to the $A\cdots H\cdots S_n$ bond, then the symmetric mode involves motion of the proton and an isotope effect is expected. Since the reactants may have slightly different structures and definitely have different solvent structures, the energy barriers for the forward and backward reactions may be in slightly different places along the potential curve and the isotope effects in k_F and k_B will not cancel. The energy difference necessary to account for the rest of the change in k_1 upon deuteration would only have to be around 0.3 kcal/mole.

The second result to consider is the effect of pressure on k_1. Huppert et al.[4] measured a_1 for aqueous 8-hydroxy-1,3,6-pyrene trisulfonate for pressures ranging from 1 to 8 kbar. Again it was assumed that $a_1 \approx k_1$. It was found that a_1 increased linearly by a factor of three over the pressure range studied. Unfortunately, the effect of increased pressure on the structure of water is not well understood,[31,38-42] making difficult predictions about changes in the microscopic rate constants that appear in our model. It has been proposed that the more compact nature of water at high pressures weakens but does not necessarily break the H-bonding in the solvent. Yet proton conductivity, and presumably k_D, increases as a function of pressure,[43] although not as sharply as the change found for k_1. The effect of pressure on k_F and k_B is not clear but it appears that k_F would have to increase relative to k_B to explain Huppert's results.

It is often stated in studies on ESPT reactions that the reactions occur only in water and not in common organic solvents such as alcohols and the formamides. While it is true that 1-naphthol does not show any evidence of ESPT in moderately basic organic solvents, the situation is quite different for the 1-naphthylammonium cation. Figures 3.12 and 3.13 show the fluorescence spectra of the 1-naphthylammonium cation in methanol, N-methylformamide, N,N-dimethylformamide, dimethylsulphoxide, acetonitrile, and, for

comparison, water in both neutral solutions and in solutions acidified so that the parent acid is the only ground-state species initially present. Emission from the basic form is clearly evident from the acidified solutions, indicating the occurrence of excited-state proton transfer. (It should be repeated here that the relative fluorescence intensities of the acidic and basic forms is not a good measure of k_1, as can be seen by examining Eqs. (15) and (16).) The reason for the difference in behavior for 1-naphthol and the 1-naphthylammonium cation is undoubtedly due to their difference in charge. 1-Naphthol is an electrically neutral acid which initially dissociates into an ion pair, while the dissociation of the 1-naphthylammonium cation does not involve charge production. The production of charged species, as in the case of 1-naphthol, can be expected to have a profound effect on all three of the microscopic rate constants that appear in our model of proton transfer. Because of the electrostatic attraction of the negatively charged conjugate base and the solvated proton, break up of the encounter complex and diffusional separation of it components will be slowed compared to positively charged acids such as the 1-naphthylammonium cation. Using statistical arguments and assuming a purely electrostatic attraction between the charged particles, Eigen[29] calculated a correction to the standard Smoluchowski diffusion equation for the rate of separation of two particles. This correction predicts that, all else remaining equal, the separation of univalent oppositely charged particles will be slower than similar but uncharged particles by the factor given in Eq. (25), valid at 20 °C,

$$\frac{k_{charged}}{k_{neutral}} = \frac{560}{\epsilon\rho\left(e^{560/\epsilon\rho} - 1\right)} \tag{25}$$

where ϵ is the solvent's dielectric constant and ρ is the "distance of closest approach" of the diffusing particles. The magnitude of this correction, relative to the value in water, is given in Table 5 for several solvents and values of ρ. As an examination of Table 5 shows, Eq. (25) is quite sensitive to the choice of ρ, making quantitative prediction difficult. For a solvent such as dimethylsulfoxide it would appear that this

effect is probably not totally responsible for the lack of ESPT from 1-naphthol. That no fluorescence from the 1-naphtholate anion is seen in DMSO implies that $k_1\tau < 10^{-3}$ where τ, the observed fluorescence decay time, is $\sim$10 ns. This further implies that $k_1(DMSO)/k_1(H_2O) < 5\times10^{-6}$, which requires from Eq. (25) that ρ <.5 Å in DMSO, an unreasonably small value.

The production of charged particles by dissociation of a neutral acid will also affect the values of k_F and k_B, relative to a similar but positively charged acid. Generally speaking, k_F will decrease and k_B increase, but quantitative predictions are not yet possible. On purely electrostatic arguments,[44] one would expect $\Delta H_F^{\ddagger}$ to increase and $\Delta H_B^{\ddagger}$ to decrease due to the charge separation in the activated complex and the encounter complex. The energy required for this charge separation will be moderated due to interactions with the solvent, but due to the close proximity of the charges in both the activated complex and the encounter complex, macroscopic solvent properties such as the bulk dielectric constant are not useful in describing the solvent influence. A more realistic treatment would have to consider the specific solute-solvent interactions that occur.

One final difference between reactions of neutral and charged acids should be mentioned. The entropy of solvation of charged particles is quite different for water and the non-aqueous solvents. In general, solvation of ions by non-aqueous solvents is accompanied by a higher degree of solvent organization relative to water.[28] This results in a larger value of $\Delta G_F^{\ddagger}$ and a smaller value of $\Delta G_B^{\ddagger}$ for acids like 1-naphthol in organic solvents, relative to their values in water. For charged acids like the 1-naphthylammonium cation, this decrease in entropy affects the parent acid, activated complex, and encounter complex to roughly the same extent. Note from Figures 3.5 and 3.8 that in H_2O $\Delta S^{\ddagger}=-6.3\pm2.6$ eu for 1-naphthol while for the 1-naphthylammonium cation $\Delta S^{\ddagger}=+1.5\pm1.0$ eu.

Several authors have attempted to utilize the fact that neutral or negativily charged acids do not undergo ESPT in non-aqueous solvents in studies on the solvent's influence on these reactions. The basic idea has been to modify the structure of water by adding

Table 5

Correction to the Smoluchowski Diffusion Equation for Univalent Oppositely Charged Particles, Relative to the Value in H_2O

ρ(Å)	Ethanol (ϵ=24.6)	Methanol (ϵ=32.7)	DMF (ϵ=36.7)	DMSO (ϵ=46.7)
0.5	5.8×10^{-14}	3.8×10^{-9}	1.4×10^{-7}	7.6×10^{-5}
1.0	4.4×10^{-7}	9.6×10^{-5}	5.6×10^{-4}	1.1×10^{-2}
1.5	8.5×10^{-5}	2.8×10^{-3}	8.7×10^{-3}	6.0×10^{-2}
2.0	1.2×10^{-3}	1.5×10^{-2}	3.4×10^{-2}	1.4×10^{-1}
2.5	5.5×10^{-3}	4.0×10^{-2}	7.5×10^{-2}	2.2×10^{-1}
3.0	1.5×10^{-2}	7.6×10^{-2}	1.3×10^{-1}	3.0×10^{-1}
4.0	5.2×10^{-2}	1.6×10^{-1}	2.3×10^{-1}	4.3×10^{-1}

DMF=dimethylformamide DMSO=dimethylsulfoxide

Figure 3.12 Fluorescence Spectra of 1-Naphthylamine and the 1-Naphthylammonium Cation in Various Solvents

The solid lines show spectra taken from solutions with $[H^+]$=0.1 M while the dashed lines show spectra taken from solutions without added acid. The peaks at ~330 nm are from the acidic form of the molecule. The peaks at ~430 nm to 450 nm are from the basic form of the molecule. For the acidified solutions, fluorescence from the basic form is an indication of ESPT. NMF is N-methylformamide.

Figure 3.12

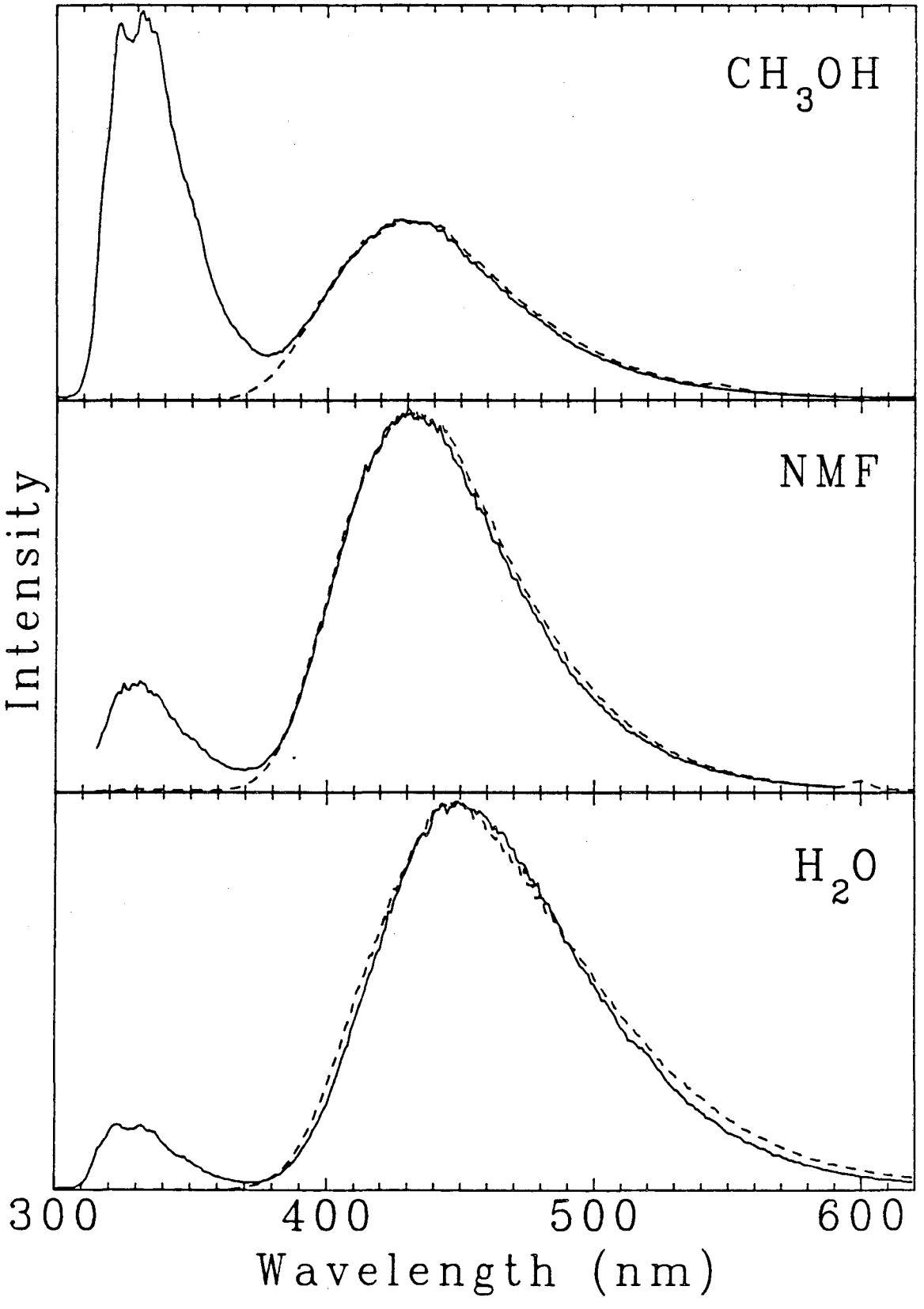

Figure 3.13 Fluorescence Spectra of 1-Naphthylamine and the 1-Naphthylammonium Cation in Various Solvents

The solid lines show spectra taken from solutions with $[H^+]$=0.1 M while the dashed lines show spectra taken from solutions without added acid. The peaks at ~330 nm are from the acidic form of the molecule. The peaks at ~410 nm to 430 nm are from the basic form of the molecule. For the acidified solutions, fluorescence from the basic form is an indication of ESPT. DMF is N,N-dimethylformamide; DMSO is dimethylsulfoxide.

Figure 3.13

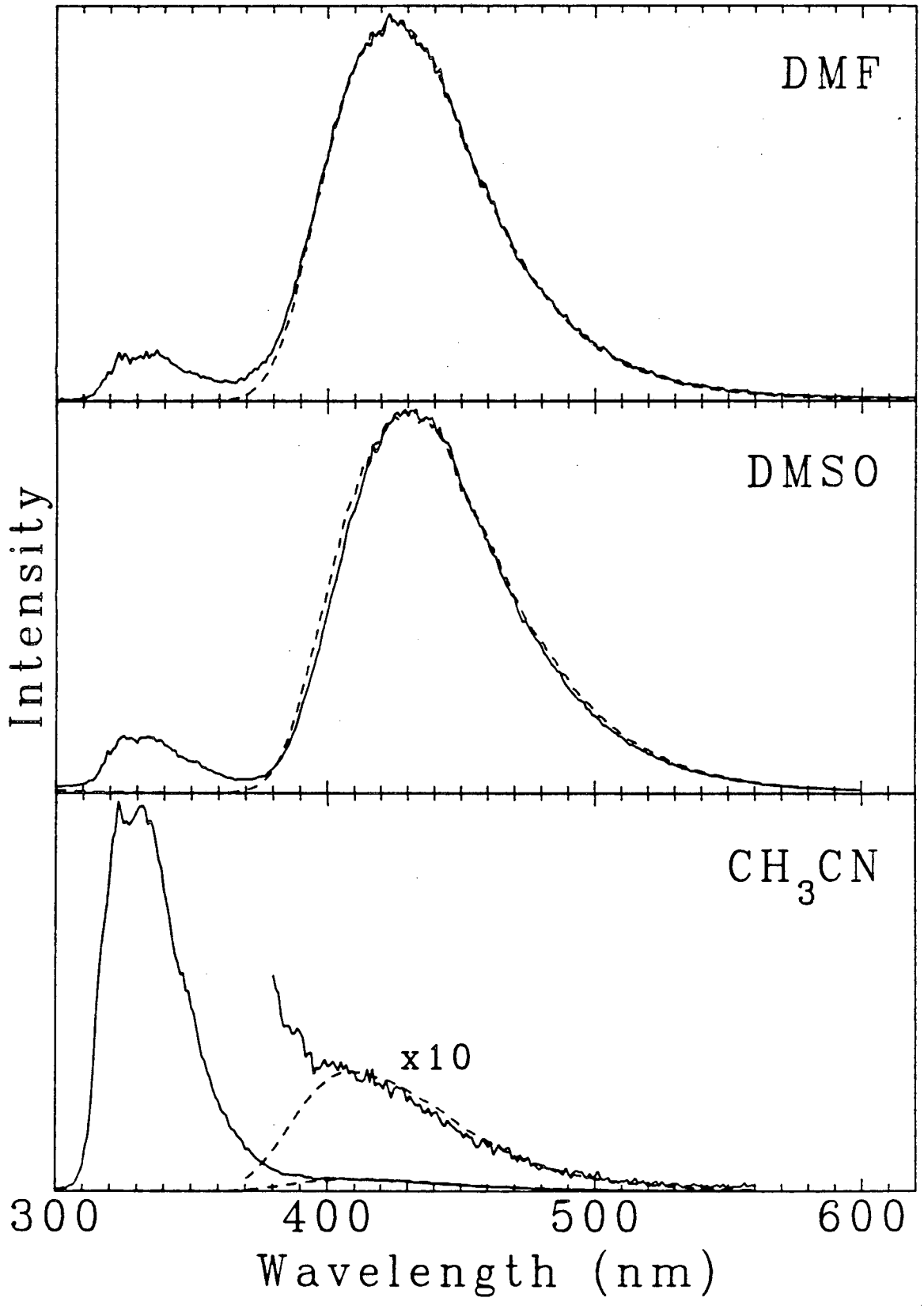

alcohols to the solutions and determine the effect on the proton transfer rate constant. Huppert et al.[3] found that for 8-hydroxy 1,3,6 pyrene trisulfonate the fluorescence risetime of the basic form decreased rapidly as ethanol was added to the solution. Huppert attributed this change to a smaller average water cluster size but was not specific as to why the size of the water clusters is important. However, the possibility exists that the observed change in the time dependence of the fluorescence is due to diffusion of water molecules up to the excited-state acid prior to the proton transfer. Robinson et al.[1,2] attempted to correct for diffusional processes in studies on ESPT from naphthols in alcohol/water mixtures. A Markov random walk method was used to account for diffusion of the water clusters. An intrinsic assumption of this method is that proton transfer will occur only with water clusters of or larger than some "critical" size. A "critical" size of 4 ± 1 water molecules was found. However, it is not clear that a valid method of determining the proton transfer rate was used, and the introduction of a "critical" cluster size is questionable. Also, there is no reason not to assume that mixed solvent clusters exist in the solution and that these mixed solvent clusters would be capable of partaking in the proton transfer reaction.

Chapter 4

Conclusion

Through an examination of the proton transfer reactions of the excited-state acids 1-naphthol and 1-naphthylammonium cation, a model for the proton transfer process that specifically includes the solvent has been developed. A cornerstone of this model is that the solvent influences the rate of the proton transfer process in three key ways: 1) the ability of the solvent to lower the energy of the dissociated proton, 2) the ability of the solvent to support the diffusional separation of the encounter complex, 3) and the thermodynamics of ion solvation for the solvent. Although the model has been useful in explaining the observed changes in the rate constants with changes in solvent properties, the real value of any model lies in its predictive abilities. In this regard it should be noted that the model presented in this thesis makes several predictions that can be experimentally tested. First, the observed deviation from the activated complex theory for 1-naphthol should also be seen in amphoprotic solvents for all acids with similar or larger proton transfer rate constants. However, in aprotic solvents such as dimethylsulfoxide and N,N-dimethylformamide even the fastest acids should obey Eq. (22). This is because these solvents do not form the H-bonded clusters that were seen as being responsible for the effect. For the same reason no salt effect, or at least a reduced salt effect, should be seen in aprotic solvents. Finally, the rate constants for charged acids such as the 1-naphthylammonium cation in different solvents should correlate with the solvent's hydrogen bonding strength, viscosity, and ability to solvate ions, particularly protons.

As a final note, it is stated in Chapter 3 that neutral acids like 1-naphthol do not, in general, undergo ESPT in moderately basic organic solvents. However, 1-naphthol does undergo ESPT in the very basic solvent triethylamine. The low dielectric constant for triethylamine (ϵ=2.4) means that the final product is undoubtedly an ion pair and the model depicted in Figure 3.9 cannot strictly apply. In addition, no ESPT occurs

for 1-naphthol in hexamethylphosphoramide, a solvent of equal basicity but much higher dielectric constant. It would appear that the proton transfer process proceeds by a different mechanism in triethylamine, and a dynamic investigation of the process would be most interesting.

References

1. J. Lee, R.D. Griffin, and G.W. Robinson; *J. Chem. Phys.* **82**, 4920 (1985).

2. S.P. Webb, L.A. Philips, J.H. Clark, J. Lee, and G.W. Robinson; in preparation.

3. D. Huppert, E. Kolodny, and M. Gutman; *Picosecond II, Springer Ser. Chem. Phys.* 242 (1980).

4. D.Huppert, A. Jayaraman, R.G. Mains, D.W. Steyert, and P.M. Rentzepis; *J. Chem. Phys.* **81**, 5596 (1984).

5. D Huppert, E. Kolodney, M. Gutman, and E. Nachliel; *J. Am. Chem. Soc.* **104**, 6949 (1982).

6. J.F. Irelano, and P.A.H Wyatt; *Adv. Phys. Org. Chem.* **12**, 131 (1976).

7. E.V. Donckt; *Prog. React. Kinet.* **5**, 273 (1966).

8. A. Weller; *Prog. React. Kinet.* **1** (1961).

9. T. Förster; *Naturwiss.* **36**, 186 (1949).

10. K. Weber; *Z. Phys. Chem.* **B15**, 18 (1931).

11. T. Förster; *Z. Electrochem.* **54**, 531 (1950).

12. A. Weller; *Z. Electrochem.* **56**, 662 (1952).

13. A. Weller; *Z. Electrochem.* **58**, 849 (1954).

14. S.P. Webb, L.A. Philips, S.W. Yeh, L.M. Tolbert, and J.H. Clark; submitted to *J. Phys. Chem.*

15. K. Tsutsumi and H. Shizuka; *Z. Phys. Chem. Neue Folge* **111**, 129 (1978).

16. K. Tsutsumi and H. Shizuka; *Z. Phys. Chem. Neue Folge* **122**, 129 (1980).

17. S. Suzuki and T. Fujii; *J. Mol. Spect.* **61**, 350 (1976).

18. M. Tichy, R. Zahradnik, J.A. Vollmin, and W. Simon; *Collect. Czech. Chem. Commum.* **37**, 962 (1972).

19. H. Shizuka and K. Tsutsumi; *Bull. Chem. Soc. Japan* **56**, 629 (1983).

20. K. Tsutsmi and H. Shizuka; *Chem. Phys. Lett.* **52**, 485 (1977).

21. C.M. Harris and B.K. Selinger; *J. Phys. Chem.* **84**, 1366 (1980).

22. T. Förster; *Chem. Phys. Lett.* **17**, 309 (1972).

23. S. Druzhinin and B. Uzhinov; *Chem. Phys.* **78**, 29 (1983).

24. S.W. Yeh; Ph.D. Thesis, University of California, Berkley, 1985

25. J.N. Demas; *Excited-State Lifetime Measurements* (Academic Press, New York, 1983).

26. L.F. Buhse; Ph.D. Thesis, University of California, Berkley, 1986

27. C. Reichart; *Solvent Effects in Organic Chemistry* (Verlag-Chemie,1979)

28. H.G. Hertz; *Angew. Chem. internat. Edit.* **9**, 124 (1970).

29. M. Eigen, W. Kruse, G. Maass, and L. De Maeyer; *Prog. React. Kinet.* **2**, 287 (1964).

30. M. Eigen; *Angew. Chem. internat. Edit.* **3**, 1 (1964).

31. B.E. Conway; *Modern Aspects of Electrochemistry* **13**, 43 (1962).

32. T. Erdey-Gruz and S. Lengyel; *Modern Aspects of Electrochemistry* **12**, 1 (1970).

33. J.Q. Searey and J.B. Fenn; *J. Chem Phys.* **61**, 5282 (1974).

34. P. Kebarle; *Thermochemical Information from Gas Phase Ion Equilibria* (Plentum Press, New York, 1975)

35. W.P. Kraemer and G.H.F. Diercksen; *Chem. Phys. Lett.* **5**, 463 (1970).

36. M.D. Newton and S. Ehrenson; *J. Am. Chem. Soc.* **93**, 4971 (1971).

37. D. Glietenberg, A. Kutschker, and M. v. Stackelberg; *Ber. Bunsenges.* **72**, 562 (1968).

38. F.H. Stillinger and A. Rahman; *J. Chem. Phys.* **61**, 4973 (1974).

39. D. Eisenberg and W. Kauzmann; *The Structure and Properties of Water* (Oxford University, London, 1969)

40. A.J. Brown and E.J. Whalley; *J. Chem. Phys.* **45**, 4360 (1966).

41. J. Jonas, T.H. DeFries, and D.J. Wilbur; *J. Chem. Phys.* **65**, 582 (1976).

42. R. Pottel and E. Asselborn; *Ber. Bunsenges. Phys. Chem.* **84**, 462 (1980).

43. M. Nakahara and J. Osugi; *Rev. Phys. Chem. Jpn.* **50**, 66 (1980).

44. I.M. Kolthoff and S. Bruckenstein; *Treatise on Analytical Chemistry* (The Interscience Encyclopedia, Inc., 1959)

This report was done with support from the Department of Energy. Any conclusions or opinions expressed in this report represent solely those of the author(s) and not necessarily those of The Regents of the University of California, the Lawrence Berkeley Laboratory or the Department of Energy.

Reference to a company or product name does not imply approval or recommendation of the product by the University of California or the U.S. Department of Energy to the exclusion of others that may be suitable.

TECHNICAL INFORMATION DEPARTMENT
LAWRENCE BERKELEY LABORATORY
UNIVERSITY OF CALIFORNIA
BERKELEY, CALIFORNIA 94720